

Comparative analysis of transcript abundance in *Pinus sylvestris* roots after challenge with a saprotrophic, pathogenic or mutualistic fungus

¹Aleksandra Adomas*, ¹Gregory Heller, ¹Åke Olson, ²Jason Osborne, ¹Magnus Karlsson, ¹Jarmila Nahalkova, ³Len van Zyl, ³Ron Sederoff, ¹Jan Stenlid, ¹Roger Finlay, ¹Frederick O. Asiegbu

¹Department of Forest Mycology and Pathology, Swedish University of Agricultural Sciences, Box 7026, Uppsala Sweden; ²Department of Statistics, Box 8203, North Carolina State University, Raleigh NC 27695 USA ³Forest Biotechnology Laboratory, Box 7247, North Carolina State University, Raleigh NC 27695, USA.

* Author for correspondence: Tel.: +46 18 67 27 98, Fax: +46 18 67 35 99, E-mail: Aleksandra.Adomas@mykopat.slu.se

Abstract

To investigate functional differences in the recognition and response mechanisms of conifer roots to fungi with different trophic strategies, *Pinus sylvestris* was challenged with a saprotrophic fungus *Trichoderma aureoviride*. The results were compared with two other separate studies investigating pine interactions with a pathogen, *Heterobasidion annosum* sensu stricto and an ectomycorrhizal symbiont, *Laccaria bicolor*. The global changes in the expression of 2109 conifer genes were assayed 1, 5 and 15 days after inoculation. Gene expression data from a cDNA microarray were analysed using the 2-interconnected mixed linear model statistical approach. The total number of genes differentially expressed as compared to un-infected control was similar after challenge with the pathogen and the ectomycorrhizal symbiont but while for *H. annosum* it increased over time, for *L. bicolor* the trend was the opposite. The inoculation of pine roots with *T. aureoviride* resulted overall in a much lower number of genes with changed transcript levels. Functional classification of differentially expressed genes revealed that the mycorrhizal fungus triggered transient induction of defence related genes. The response and induction of defence against the pathogen was delayed and the magnitude increased over time. The results indicate that there were specific transcriptional responses of conifer roots challenged with mutualistic, saprotrophic or pathogenic fungi. This suggests that pine trees are able to recognize all three organisms and specifically distinguish whether they are pathogenic, neutral or beneficial microbial agents.

Key words: microarray, mycorrhiza, pathogen, *Pinus sylvestris*, recognition, saprotroph.

Introduction

Forest trees, like other plants, are exposed to a diverse array of microbes including fungi, bacteria and viruses at every stage of their life cycle. While mutualistic associations are favourable to both of the partners and interactions with

saprotrophs are usually neutral, interactions with pathogens are often detrimental and may even lead to death of the plant host. Encounters between plant cells and microorganisms can trigger a range of highly dynamic plant cellular responses. A major requirement for induction of any form of host response reaction is the recognition of the presence of an invader. Activating the defence mechanisms is an energy consuming process, therefore a critical distinction must be made by the plant between pathogenic and non-pathogenic microorganisms, the physiological and molecular basis of which is still poorly understood (Asiegbu et al. 1999a; Hahlbrock et al. 2003).

Many of the microbes associated with forest trees and plants have an important impact on plant ecology and evolution and are also key components in maintaining vital ecosystem processes. Some of these microbes cause diseases in plants and trees while others prevent diseases or enhance plant growth. In trees alone, fungi cause several thousands of different diseases including the root and butt rot caused by *Heterobasidion annosum* sensu stricto (Fr.) Bref. (Asiegbu et al. 2005). The majority of the invading pathogens are recognized by the host, inducing a rapid defence response. If the defence fails, a disease develops, ultimately leading to death of the host plant. At the other extreme, beneficial mutualistic organisms play important and economically significant roles in plant growth as well as in nutrient cycling. Ectomycorrhizal fungi (ECM) form mutualistic associations and colonise the vast majority of tree roots in boreal forests (Smith and Read 1997). The fungal partner provides the plant with several benefits, including an enhanced ability to absorb water and important elements such as phosphorus and nitrogen (Smith et al. 1994) and improved tolerance of stress arising from soilborne root pathogens (Duchesne et al. 1987) and heavy metals (Galli et al. 1994). Formation of ectomycorrhizal roots involves both structural and metabolic integration which is achieved through development of a fungal mantle and Hartig net without evoking persistent host defence reactions (Martin et al. 2004; Tagu and Martin 1996). Development appears to involve highly coordinated molecular processes that are the result of pre-established genetic programs in both partners (Johansson et al. 2004; Martin et al. 2004; Tagu et al. 1993).

Although it is often assumed that saprotrophic fungi do not interact directly with plants (Boddy 1999), they are fundamentally important in decomposition, energy flow and nutrient cycling, particularly in forest ecosystems. However, recent research also suggests that there might be some functional overlap between fungi with different primary trophic strategies. Mycorrhizal symbioses have been alternatively viewed as stable derivatives of ancestral antagonistic interactions or as inherently unstable, reciprocal parasitisms, but recent phylogenetic analyses of free-living and mycorrhizal homobasidiomycetes (Hibbett et al. 2000) suggest that mycorrhizal symbionts have evolved repeatedly from saprotrophic precursors. Moreover, there may also have been multiple reversals to a free-living condition, supporting the view that mycorrhiza are unstable, evolutionarily dynamic associations. A recent study by Vasiliauskas et al. (2007) provides evidence of the ability of a wood decaying fungus to colonise fine roots of tree seedlings.

Numerous studies have investigated plant responses to mutualistic (Johansson et al. 2004; Manthey et al. 2004) or pathogenic (Bar-Or et al. 2005; McFadden et al.

2006) colonisation but very few have compared responses in the same plant (Asiegbu et al. 1999a; Guimil et al. 2005; Mohr et al. 1998; Salzer et al. 2000; Weerasinghe et al. 2005). Most comparative work has been done on crop and model plants using arbuscular mycorrhiza fungi as a mutualistic organism and looking at expression of few selected defence-related genes (Mohr et al. 1998; Salzer et al. 2000). Global gene expression analysis offers a possibility to unravel the molecular basis of the distinction made by plants between pathogenic and non-pathogenic microorganisms. Transcriptome analyses and cDNA microarrays have been successfully employed to investigate plant responses to biotic and abiotic stresses: drought, cold and salt stress (Fowler and Thomashow 2002; Kawasaki et al. 2001; Ozturk et al. 2002; Seki et al. 2002); relatively little work has been conducted on forest trees (Gu et al. 2004; Smith et al. 2004; Watkinson et al. 2003). Use of ectomycorrhizal, pathogenic and saprotrophic fungi, coupled with large scale transcriptome analysis offers new possibilities to identify genes involved in recognition and regulation in different types of plant-fungal interactions.

The present study is part of a series investigating the response of conifer tissues at various stages of development to the presence of trophically diverse fungal species. The ultimate objective is to characterise the temporal patterns of host responses to these different fungi and to improve our understanding of the mechanisms underlying recognition and defence. Here we present an analysis of transcript profiling of *Pinus sylvestris* roots challenged with a saprotroph *Trichoderma aureoviride* Rifai and compare the results to transcript profiles from interactions of pine roots with two other fungi, a pathogen, *H. annosum* s.s. (Adomas et al., in press) and an ectomycorrhizal fungus, *Laccaria bicolor* Maire (Orton) (Heller et al., in preparation).

Materials and Methods

Host plant, pathogen and root inoculation

Pinus sylvestris seeds (provenance Eksjö, Sweden) were surface sterilised with 33% H₂O₂ for 15 min, rinsed in several changes of sterile distilled water, sown on 1% water agar and incubated at 18°C with a photoperiod of 16h. After 14 days, the resulting seedlings were used for inoculation. *Trichoderma aureoviride* (isolate A361, courtesy of G. Daniel, Sweden) was maintained on Hagem agar (Stenlid 1985) at 20°C. The mycelium used for inoculation was obtained from cultures grown in liquid Hagem medium for 14 days under static conditions. The mycelium was washed with sterile water and subsequently homogenized for 60 seconds in a sterile Waring blender. Ten seedlings of *P. sylvestris* were transferred to wet, sterile filter paper placed on 1% water agar in Petri dishes. The roots were inoculated with 1 ml of the mycelial homogenate and covered with a second moist sterile filter paper. The plate was sealed with parafilm and the region of the dish containing the roots was covered with aluminium foil. The seedlings were then incubated at 18°C with a photoperiod of 16h. Control plants were mock-inoculated

with 1 ml sterile distilled water. The roots of 100 seedlings of either infected or control plants were harvested at 1, 5 and 15 days post inoculation (d.p.i.), ground in liquid nitrogen and stored at -80°C prior to RNA extraction. There were three biological replications. Pine roots were also inoculated with *Heterobasidion annosum* s.s. (isolate FP5, courtesy of K. Korhonen, Finland) (Adomas et al., in press) or *Laccaria bicolor* (courtesy of A. Tunlid, Sweden) (Heller et al., in preparation).

Preparation of samples for scanning and transmission electron microscopy (SEM and TEM)

Five seedlings were harvested 1, 5 and 15 d.p.i. Root samples (10 mm from the tip) were excised from each plant, prefixed in 3% (v/v) glutaraldehyde, washed in phosphate buffer (3 x 10 min) and post-fixed for 3h in 1% (w/v) osmium tetroxide. After washing in distilled water (4 x 15 min), roots were dehydrated using a 10 step ethanol series (i.e 10%, 20%, 30% to 100%), then an ethanol-acetone series (3:1, 2:2, 1:3, pure acetone, 10 min each), and dried using a polaron critical point dryer. Samples were mounted on stubs using double sided adhesive tape and coated with gold using a Polaron E5000 sputter coater. Roots were observed using Hitachi S-4500 SEM operated at 15 kV. Samples for TEM were prepared as previously described (Asiegbu et al. 1994).

Tissue preparation for determination of cell death by fluorescence microscopy

Seedlings were harvested at 5 d.p.i. Nuclear staining was carried out as described by Henry and Deacon (1981). Briefly, excised root regions (first 10mm from root tip) were hydrolysed in 3% HCl in 95% ethanol (5 min at room temperature), washed twice in phosphate-citrate buffer, pH 3.8, stained with 0.001% acridine orange in phosphate buffer for 15 min at room temperature and rinsed twice in phosphate-citrate buffer. Root pieces were examined under a Leitz Orthoplan fluorescence microscope with excitation filter I2: BP 450–490. The number of fluorescent nuclei within a microscope field of view using a x40 objective was counted for both infected and control roots (3 fields of view per root in a total of 10 roots per sample).

cDNA library construction from *Pinus taeda* and characteristics of ESTs analysed

The ESTs (expressed sequence tags) used for this study were obtained from six cDNA libraries of *P. taeda* representing different developmental stages in wood formation (<http://biodata.cgb.umn.edu/>) (Kirst et al. 2003). The 2109 ESTs on the array were manually classified by reference to the *Arabidopsis thaliana* database at <http://pedant.gsf.de> and the Genbank. The best hit from the BLAST search was utilized for grouping the cDNAs into functional categories (see Stasolla et al. 2003).

Microarray preparation

Probe preparation was performed in accordance with earlier published procedures (Kirst et al. 2003; Stasolla et al. 2004; Stasolla et al. 2003). Briefly, DNA from each of 2109 ESTs was printed onto amino-silane coated CMT-GAPS slides (Corning Inc; Corning, NY, USA) in four replications for hybridizations performed at 1 d.p.i. and in two replications at 5 and 15 d.p.i. using a Lucidea Array Spotter (Amersham Biosciences, USA). After printing, the DNA was cross-linked using 250 mJ of UV-C radiation. The slides were subsequently heated at 75°C for 2 hrs, stored in slide containers in the dark at room temperature and used within 10 days.

cDNA labelling and hybridisation

Total RNA was isolated from infected and control roots of *P. sylvestris* seedlings as described by Chang et al. (1993). The cDNA was synthesised from the same amount of RNA (1 µg) using SMART™ PCR cDNA synthesis kit (Clontech, USA). The cDNA generated from infected and control roots at each point was reciprocally labelled with Cy3 and Cy5-dUTP (Perkin Elmer, USA) using a Klenow method. Labelling, hybridization, and stringency washes followed the protocol from North Carolina State University (Brinker et al. 2004). The experimental design involved comparison of inoculated versus un-inoculated samples at each time point: 1, 5 or 15 d.p.i. Taking into consideration dye-swaps and technical replicates, each sample was hybridized six times and there were a total of 72 data points for each gene on the array at 1 d.p.i. and 36 at 5 and 15 d.p.i. Slides were scanned with a ScanArray 4000 (GSI Lumonics, Oxnard, CA USA) and raw, non-normalized intensity values were registered using Quantarray software (GSI Lumonics).

Statistical analysis

The statistical significance of changes in transcript abundance was estimated using two successive mixed models as described by Wolfinger *et al.* (2001) and Jin *et al.* (2001).

$$\text{Log}_2(Y_{ijkmg}) = L_i + T_j + D_k + LT_{ij} + LD_{ik} + TD_{jk} + S_l + B_m + SB_{lm} + SD_{lk} + BD_{mk} + \epsilon_{ijkmg} \quad (\text{M1})$$

$$R_{ijkmg} = L_{ig} + T_{jg} + D_{kg} + LT_{ijg} + LD_{ikg} + TD_{jkg} + S_{lg} + BS_{img} + SD_{lkg} + \xi_{ijkmg} \quad (\text{M2})$$

Model M1 is used to normalize all the data, and Model M2 is then fit separately to one gene at a time. Y_{ijkmg} represents the raw intensity measurement from the i^{th} cell line (batch), the j^{th} treatment, the k^{th} dye channel, the l^{th} slide, and the m^{th} block in the array for the g^{th} gene. R_{ijkmg} represents the residual computed as $\text{Log}_2(Y_{ijkmg})$ minus the fitted effects from (M1). The symbols L, T, D, S, and B represent effects of cell line, treatment, dye, slide and block effect, respectively. Double symbols represent corresponding interaction effects. The terms S, B, SB, SD, and BD in (M1) are considered to be random effects, as are terms S, BS, and SD in (M2); others are fixed effects, and ϵ and ξ are stochastic errors. All the random effect terms including the errors are assumed to be normally distributed with mean 0 and effect-specific variance components. Estimates of fold changes for each gene and their statistical significance are based on fitted values from (M2). Many

transcript abundance expression changes less than two-fold were statistically significant (Jin et al. 2001); however, some compression in these estimates is likely, as shown in later comparison with RT-PCR. To conservatively ensure a false positive rate of 0.01, a p-value cutoff was set at the Bonferroni value of $0.01/2109 = 4.5 \times 10^{-6}$, as suggested by Wolfinger *et al.* (2001).

Real-time quantitative RT- PCR analysis of gene transcription

Verification of expression of selected genes was performed using real-time quantitative RT-PCR. Total RNA was extracted from seedlings infected independently from the microarray experiment and there were three biological replicates. The RNA (2 µg) was digested with deoxyribonuclease I (Sigma, Sweden) according to manufacturer's instructions and further quantified using Quant-iT RiboGreen RNA Assay Kit (Molecular Probes, Invitrogen, Sweden). Equal amounts of RNA (1 µg) were reverse transcribed with M-MLV reverse transcriptase (Invitrogen, Sweden) following the manufacturer's instructions. Specific primer pairs (see Supplementary materials Table S1) were designed against each gene with amplicons ranging from 50 to 94 bp. Relative transcript abundance was measured using an ABI Prism 7700 Sequence Detection System (Perkin-Elmer Applied Biosystems, Sweden) and SYBR Green PCR Master Mix (Applied Biosystems) according to manufacturer's recommendations. Transcript levels were calculated from three technical replicates using the standard curve method (User Bulletin #2, ABI Prism 7700 Sequence Detection System, Applied Biosystems). For preparation of the standard curve, plasmids of interest were extracted with QIAprep[®] Spin Miniprep kit (Qiagen, Sweden). The plasmid DNA concentration was determined using Quant-iT PicoGreen dsDNA Kit (Molecular Probes, Invitrogen, Sweden). A serial dilution of each plasmid was prepared, including 10^6 , 10^5 , 10^4 , 10^3 and 10^2 copies/µl and real-time RT-PCR was performed. The absolute quantity of the product in each sample was calculated from the standard curves and was normalized against the total amount of RNA as described previously (Hashimoto et al. 2004; Silberbach et al. 2005).

Sequence analysis

Genes identified as differentially expressed during infection of *P. sylvestris* roots with *T. aureoviride* were subjected to contig analysis with SeqMan (MegAlign[™] expert sequence analysis software, version 5.05).

Results

Microscopical analysis of the root colonisation

Pinus sylvestris seedling roots were inoculated with homogenized mycelia of *Trichoderma aureoviride* (saprotroph) and the observations were compared to those from similar studies conducted using either a pathogenic fungus *Heterobasidion annosum* or a mycorrhizal fungus *Laccaria bicolor* (Table 1). Examination of roots revealed adhesion of hyphal material within 30 minutes of

exposure. At 1 day post inoculation (d.p.i.) no visible symptoms, such as necrotic browning or hypersensitive reaction (HR) were documented on the roots in any of the interaction types. *Trichoderma aureoviride* formed a network of hyphae on the root surface within 1 day post inoculation (Fig. 1a). At 5 d.p.i. dichotomously branched hyphae and spores of the fungus were observed (Fig. 1c). Although the fungus was able to enter the protodermis and epidermis (Fig. 1b) there was no evidence of appressorium formation (Fig. 1d) or hyphal penetration of root cells (Fig. 1e-f). No detectable necrosis or loss of turgidity occurred in seedlings inoculated with the saprotroph (*T. aureoviride*) or the mycorrhizal fungus (*L. bicolor*). Examination of the roots revealed evidence of emerging lateral roots colonised by *L. bicolor* at 15 d.p.i. (Heller et al., in preparation). Roots which were exposed to *H. annosum* developed typical necrotic browning and intracellular hyphal penetration occurred between 5 and 15 d.p.i. (Table 1).

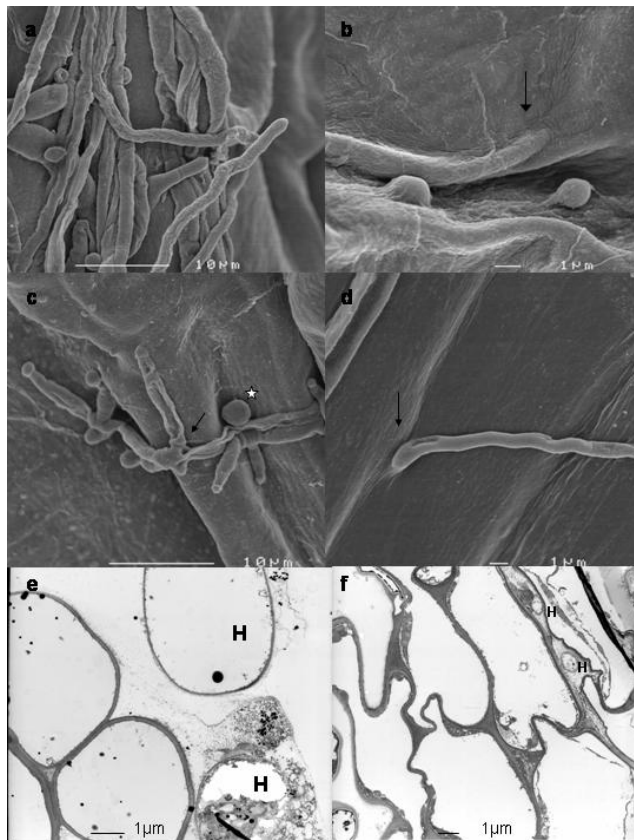


Fig. 1. Scanning electron microscope (SEM) photographs of inoculated *P. sylvestris* roots showing development of *T. aureoviride*: a) adhesion and actively growing hyphae on the root surface at 1 d.p.i.; b) hyphae attempting to penetrate the root via crevices (arrow); c) dichotomously branching hyphae (arrow) and spores (star) at 5 d.p.i.; d) hyphal tip developing on the root surface (arrow). Transmission electron microscopy (TEM) documenting e) presence of the hyphae (H) outside the root in the proximity of epidermis and f) hyphae (H) within protodermis and epidermis at 15 d.p.i. Bar represents 1, 10 or 100 μm.

Cell death in *P. sylvestris* roots challenged with the saprotroph *T. aureoviride* compared with responses to pathogenic (*H. annosum*) or ectomycorrhizal fungus (*L. bicolor*)

A cell death assay was used to evaluate the extent of host recognition of the invading fungus. The assay was conducted at 5 d.p.i when all three fungi had adhered and established on the root surface. The result showed a higher proportion of dead cells in the pathogenic (55%) interaction compared to the saprotrophic (0%) or ectomycorrhizal associations (5%) (Fig. 2).

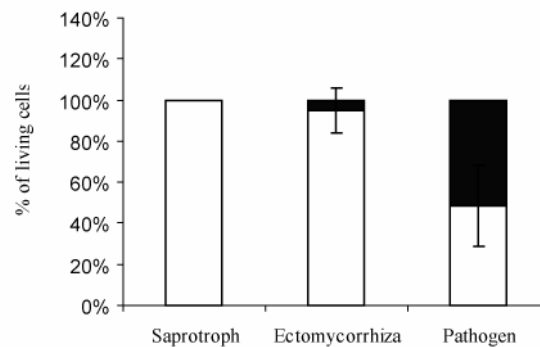


Fig. 2. The percentage of living (white) and dead (black) cells in *P. sylvestris* roots challenged with a saprotroph (*T. aureoviride*), a pathogen (*H. annosum*) or an ectomycorrhizal fungus (*L. bicolor*) at 5 d.p.i. as compared to un-inoculated control.

Transcript profiling of *P. sylvestris* root tissues challenged with *T. aureoviride*

To analyse changes in gene transcript levels in *P. sylvestris* root tissues inoculated with *T. aureoviride*, a cDNA microarray containing 2109 ESTs from *P. taeda* was used. Mixed model analysis identified a total of 41 ESTs differentially expressed with a fold change greater than 1.2 or below -1.2 (Table 2). Pairwise comparison of the infected seedlings versus un-inoculated controls distinguished a total of 23, 2 and 6 ESTs significantly up-regulated at 1, 5 and 15 d.p.i., respectively. The number of ESTs with significantly decreased transcript levels was 4, 0 and 6 at 1, 5 and 15 d.p.i., respectively. The expression pattern was unique for each group and genes up- or down-regulated at one time point were not differentially expressed at other time points. Contig analysis of those sequences showed that 3 contigs were represented by two ESTs each. The fold changes of both ESTs constituting each contig had similar fold change values (Table 2). Ultimately, there were 38 unique genes differentially expressed by *P. sylvestris* in response to *T. aureoviride*. Gene expression in major functional categories is shown in Table 2. At 1 d.p.i. the highest number of up-regulated genes belonged to two functional categories: cell rescue/defence (antimicrobial peptide, thaumatin and immunophilin) and transcription. The two genes up-regulated at 5 d.p.i. were classified as transport and development related. Genes up-regulated at 15 d.p.i. grouped mostly into the functional class of metabolism. Genes down-regulated at

1 or 15 d.p.i. were distributed among different functional categories. A number of genes differentially expressed in response to challenge with *T. aureoviride* had an unknown function.

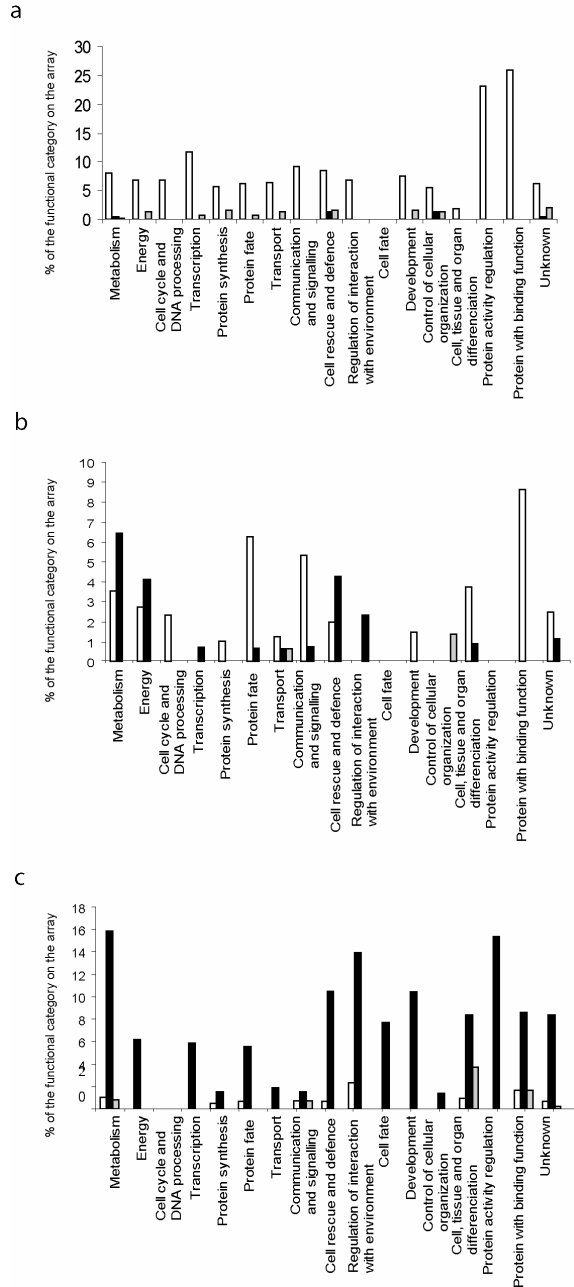


Fig. 3. The percentage of genes relative to functional classes on the array up-regulated by *P. sylvestris* in response to challenge with a pathogen (*H. annosum*) [black], an ectomycorrhiza symbiont (*L. bicolor*) [white] or a saprotroph (*T. aureoviride*) [grey] at a) 1; b) 5 and c) 15 d.p.i

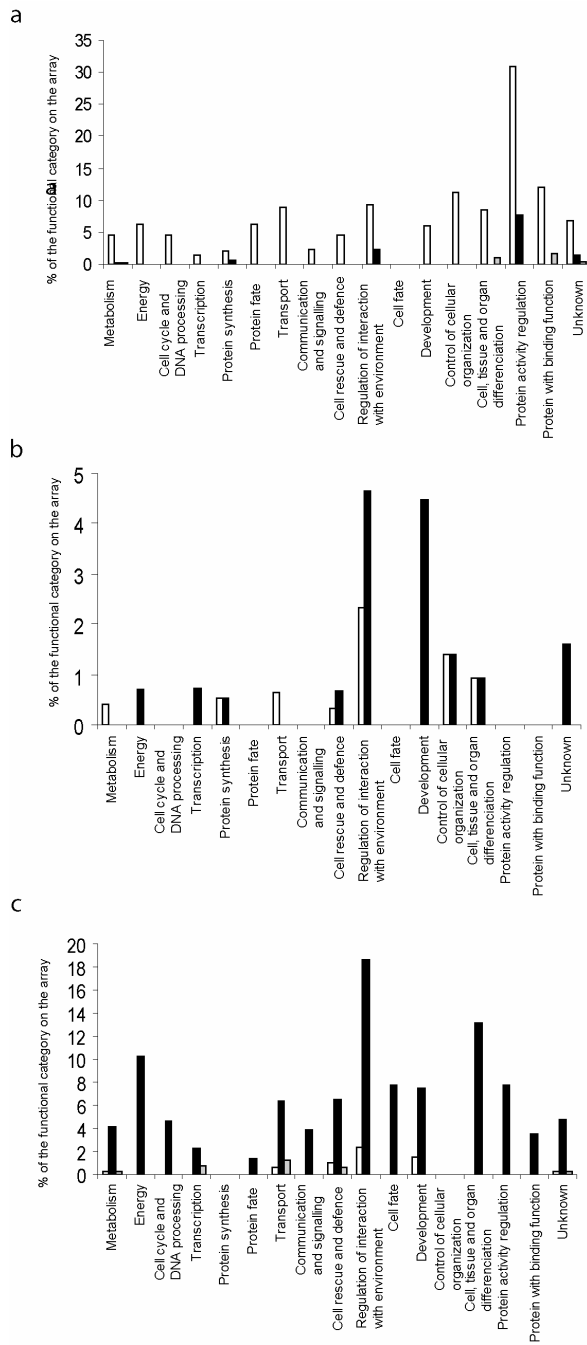


Fig. 4. The percentage of genes relative to functional classes on the array down-regulated by *P. sylvestris* in response to challenge with a pathogen (*H. annosum*) [black], an ectomycorrhiza symbiont (*L. bicolor*) [white] or a saprotroph (*T. auroviride*) [grey] at a) 1; b) 5 and c) 15 d.p.i

Real-time RT-PCR validation of expression of selected genes in *P. sylvestris* roots challenged with *T. aureoviride*

To evaluate the validity of the microarray results, the expression patterns of six genes were further examined by real-time RT-PCR. The fold changes determined by real-time RT-PCR were usually higher but otherwise consistent with the microarray data (Table 3). For example, in the array, a fold change of -1.2 was recorded for endo-beta 1-4 glucanase with a corresponding value of -18.0 in the real-time RT-PCR. Similarly, zinc finger protein with a fold change value of 1.3 in the array had a value of 1.6 in the real-time RT-PCR experiment. The distribution of copy numbers within the biological replicates in the control and challenged pine roots is presented in Supplementary materials (Fig. S1a-f).

Comparative transcript profiling of *P. sylvestris* genes differentially expressed after challenge with a pathogen, a saprotroph or a mutualist - gene numbers

The transcript profiling of the response of *P. sylvestris* to colonisation by the saprotrophic fungus (*T. aureoviride*) was compared to earlier data on the response of the same type of tissue to pathogenic or mycorrhizal fungi. The number of genes differentially expressed by pine roots in response to challenge with the three different fungi at 1, 5 and 15 d.p.i. is presented in Table 4 (the complete list of genes is presented in Supplementary Table S2). It was observed that the total number of genes differentially expressed was similar after challenge with the pathogen and the mutualist (ca 17% of all the genes on the array) but, while for *H. annosum* this number increased over time, for *L. bicolor* the trend was the opposite (Table 4). The inoculation of pine roots with *T. aureoviride* resulted in an overall much lower number of genes with changed transcript levels (2% of the genes on the array). The number of genes differentially expressed during the saprotrophic interaction decreased at 5 d.p.i. and then increased at 15 d.p.i., although to a level much lower than at 1 d.p.i. (Table 4). At any single time point there was no overlap in gene expression in the response of the pine roots between the three treatments. Roots inoculated with the pathogen or the saprotroph shared only two up-regulated genes at 1 d.p.i. (antimicrobial peptide and thaumatin) and two down-regulated genes at 15 d.p.i. (metallothionein and non-specific lipid transfer protein). The mycorrhiza and saprotroph treatments shared three genes which were down-regulated at 1 d.p.i. (nuclear RNA binding protein and unknown proteins) and two genes up-regulated at 15 d.p.i. (calcium binding protein and glycine-rich protein homolog). The overlap between pathogen and mycorrhiza treatments was more significant: at 1 d.p.i. there were three genes up-regulated (histone H3 and hypothetical proteins) and six genes down-regulated (arabinogalactan protein, aquaporin and unknown proteins); at 5 d.p.i. one gene (NADH-glutamate synthase) was up-regulated and one (gibberellin regulated protein) down-regulated; and at 15 d.p.i. nine genes had increased transcript levels (peroxidase, 40S ribosomal protein, S-adenosylhomocysteinase, heat shock protein 70, early response to drought, endoxyloglucan transferase and unknown), while five had decreased transcript levels (aquaporin, abscisic acid/water

stress/ripening inducible, membrane intrinsic protein Mip-2, MtN21 nodulin protein-like and disease resistance protein).

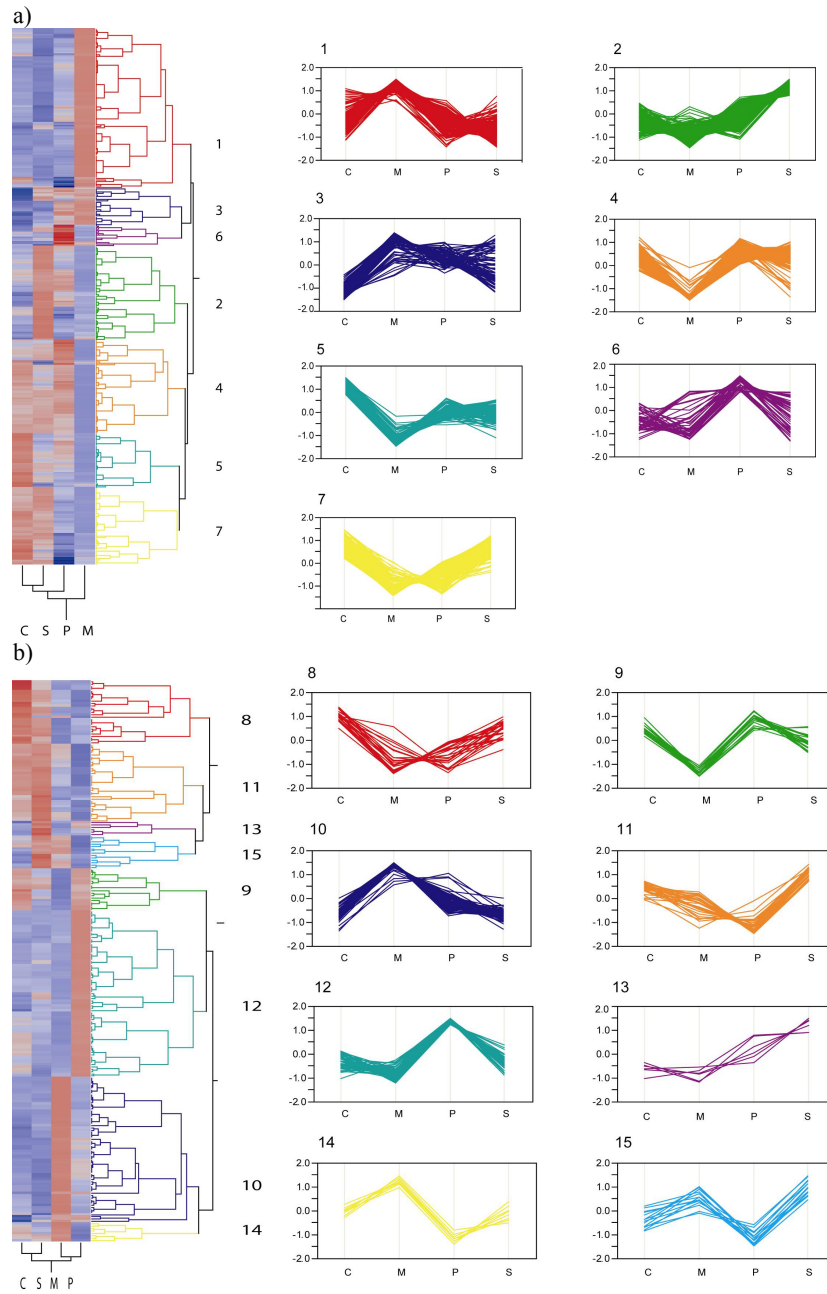
Comparative functional analysis of *P. sylvestris* genes differentially expressed in response to challenge with either a saprotrophic, pathogenic or mutualistic fungus

The gene expression in major functional categories is shown in Fig. 3 and 4 as a percentage of all the genes belonging to the given category present on the array. The number of genes differentially expressed by *P. sylvestris* in response to the saprotroph was lower than 4% of any functional category and has been discussed above. At 1 d.p.i. the most prevalent genes up-regulated in response to the mycorrhizal fungus belonged to the functional categories of protein activity regulation, protein with binding function and transcription (Fig. 3a). The highest number of genes down-regulated in response to the mycorrhizal fungus was related to protein activity regulation (Fig. 4a). Interestingly, the same functional group was predominantly down-regulated by pine roots in response to the pathogen at 1 d.p.i. (Fig. 4a). At 5 d.p.i. the interaction involving *L. bicolor* resulted mostly in an increase of the transcript levels of genes belonging to the functional class of proteins with binding functions, protein fate and communication and signalling. Similarly, pine roots responded to the pathogen with increased transcription of genes with functions important in metabolism, energy and cell rescue and defence (Fig. 3b). Two of the most abundant groups of transcripts that decreased after pathogen challenge coded for proteins related to regulation of interaction with environment and development. At 5 d.p.i. genes down-regulated in response to *L. bicolor* did not exceed 3% of any functional group present on the array (Fig. 4b). At 15 d.p.i. the *P. sylvestris* response was specific only to the pathogen; mycorrhiza did not cause a significant change in the gene expression (Fig. 3c and 4c, Table 4). Among the genes with transcript levels that increased after *H. annosum* infection, most belonged to the functional groups associated with metabolism, protein activity regulation, regulation of interaction with environment and cell rescue/defence (Fig. 3c). Most of the genes down-regulated in response to the pathogen were related to regulation of interaction with environment, cell, tissue and organ differentiation and energy (Fig. 4b).

Coordinated gene regulation of *P. sylvestris* root tissues in response to saprotrophic, pathogenic or mutualistic fungal colonisation

A hierarchical clustering was performed on ESTs indicated by the mixed model analysis as significantly expressed (Fig. 5) (see also Supplementary Table S2). All the genes were grouped into regulatory patterns. The most striking feature of the global expression pattern at 1 d.p.i. was the clear response to the ectomycorrhizal fungus (Fig. 5a). A small number of genes with high expression levels overlapped between the mycorrhiza and the pathogen treatment and between the mycorrhiza and saprotroph treatment (cluster 3). The expression profile of control uninfected pine tissues was most closely related to the saprotroph challenged roots. The host

reaction to the pathogen was not specific, except for a number of genes belonging to cluster 6 (Fig. 5a).



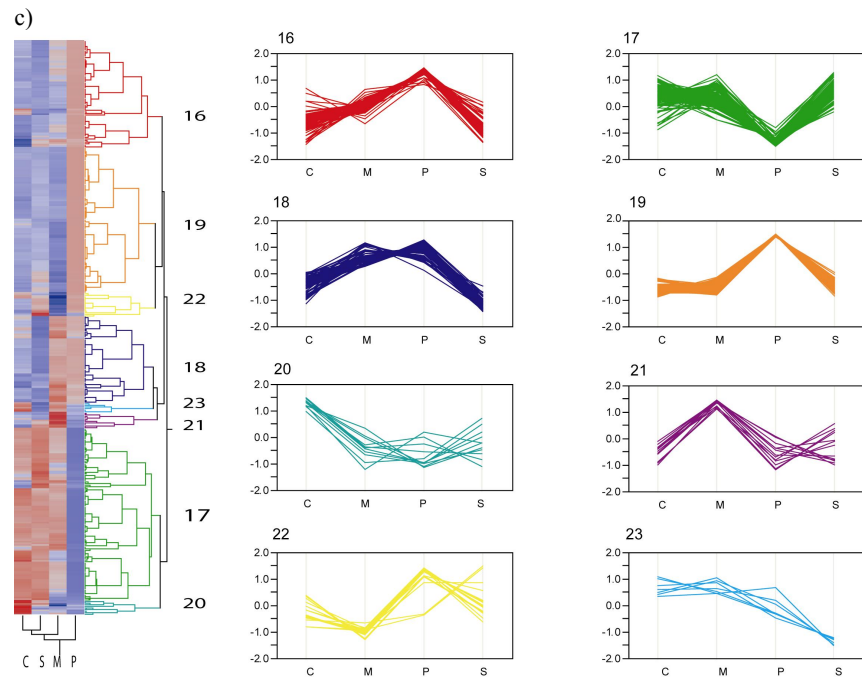


Fig. 5. Hierarchical clustering illustrating groups of *P. sylvestris* genes coordinately expressed in response to inoculation with the pathogen *H. annosum* (P), the ectomycorrhiza *L. bicolor* (M) or the saprotroph *T. aureoviride* (S) at a) 1, b) 5 and c) 15 d.p.i. Each row illustrates expression profile of each of significantly expressed genes (identified by mixed model analysis) (red-blue colour - high-low expression). All the differentially expressed genes were divided into 23 regulatory patterns, indicated by the numbers 1-23 (see also Supplementary Table S2).

The global expression pattern at 5 d.p.i. was remarkable due to the clear distinction between all three interactions (Fig. 5b). The genes specific for the pathogen interaction grouped in cluster 12 and those specific for the mycorrhiza interaction in clusters 10 and 14. The saprotrophic interaction was clearly different from the other two but very similar to the un-inoculated control. Cluster 9 was represented by genes with similar expression levels in the control and pathogen infected roots and pattern 15 – in saprotrophic and mycorrhizal interaction (Fig. 5b). At 15 d.p.i. there was a shift in the global expression pattern towards a pine response that was specific to the pathogen and fairly unspecific to the saprotroph and mycorrhiza. Only a small number of up-regulated genes were exclusively associated with the mycorrhiza treatment (cluster 21) (Fig. 5c). A number of genes similarly expressed in response to the challenge with pathogen and mycorrhiza grouped together in cluster 18.

Discussion

In the present study, microarray analysis was used to examine conifer root responses to colonisation by a saprotrophic fungus, *T. aureoviride*. The results

were compared to similar studies conducted with a mutualist, *L. bicolor* and a pathogen, *H. annosum*. The three fungal species differ significantly in their strategies for obtaining nutrients and associating with plant roots. Saprotrophs, interacting mostly only with the exterior parts of roots, thrive on dead organic matter and are seldom reported to cause disease. Ectomycorrhizal (ECM) fungi on the other hand are facultative biotrophs relying on their host for the supply of carbon sources and can penetrate host tissues but only intercellularly. *Heterobasidion annosum* is a necrotrophic pathogen with a life cycle switching between two phases: parasitic and then, later on when the tree is killed, saprotrophic. Unlike the saprotroph and the ECM fungus, *H. annosum* is capable of intracellular invasion into host tissues (Table 1).

Usually, a plant response to microbial invasion consists of both constitutive and inducible defences (Dixon and Lamb 1990; Pearce 1996). The most pronounced inducible defence at the macroscopic level is necrosis. In this study, the host response in terms of necrotic cell death was found to be weaker in plants challenged with both saprotrophic and ectomycorrhizal fungi compared to those challenged with the pathogen. Our results indicate that the pathogen mediated compatibility reactions leading to necrotic cell death do not occur in the case of ectomycorrhiza or saprotrophs. Cell death is a normal physiological process during tissue development but induction during microbial invasion may have fundamental ecophysiological implications depending on the lifestyle of the pathogen (Greenberg 1996). Obligate parasites that depend on living host cells may be restricted from further growth by the hypersensitive-response related cell death but other pathogens (necrotrophs) benefit from the release of nutrients from dead cells (Greenberg 1997). In this study, prolonged exposure to *H. annosum* led to loss of root turgidity and death suggesting that necrotic cell death did not function as a mechanism of resistance to this necrotrophic parasite.

The exact mechanisms by which plants are able to distinguish between pathogenic and non-pathogenic fungi are still largely unknown. The molecules involved in recognition have not been thoroughly examined in forest trees. The high correlation of transcript levels for the same tissues between *P. sylvestris* and *P. taeda* ($r=0.93$) permitted differential screening to be done using the *P. taeda* cDNA arrays with RNA made from Scots pine roots (van Zyl et al. 2002). For this analysis, arrays were constructed with 2109 cDNA clones from *P. taeda*. At the transcriptome level, the pine seedlings showed a transient uncoordinated weak defence response during challenge with either the saprotroph or mycorrhizal fungi. Over time, the host responses were shown to be stronger towards the pathogen. Comparing pathogenic interaction with non-pathogenic models, it was expected that pine roots would initially respond more dramatically to the pathogen than to the other fungi. Instead, a lower number of genes was found to be differentially expressed in the pathogenic interaction at the early stage of interaction compared to mycorrhizal and saprotrophic associations. The delayed plant response to the pathogen infection may be attributed to a lack of information possessed by the plant about the nature of the attack during the initial phase of infection. Since the timing of the host response seems to be crucial, the ability of *H. annosum* to avoid immediate recognition during the initial stages of interaction may allow it to

penetrate the host tissues before the defence response can be induced. This can be seen as a part of the strategy of a successful pathogen.

In terms of recognition several studies have shown that fungi elicit active defence mechanisms via their surface traits, secretion or activities (Jones and Takemoto 2004). A series of studies of different rhizobia-legume associations has shown that saccharides may play an important role as signals to the host plants (Campbell et al. 2002; Dunlap et al. 1996). Interestingly, saccharides from the soybean symbiont *Bradyrhizobium japonicum* share some structural features with those derived from the cell wall of phytopathogenic oomycete *Phytophthora sojae*. It has been suggested that the host induction or suppression of defence reaction might be regulated by the ratio of plant receptor occupancy by the two signalling compounds involved (Mithofer 2002). The molecular basis for recognition of fungal pathogens also stems from the binding of host plant lectin-like molecules to sugar haptens on the surface of the invader and vice versa (Mazau et al. 1987). Unfortunately, in gymnosperms host specificity and the mechanisms underlying the process of recognition and onset of defence reactions are poorly understood.

Based on the results, we hypothesized that the location of a polysaccharide, chitin, within the cell walls of the different fungi could be an important factor in our understanding of how trees distinguish between harmful and non-pathogenic organisms. Our presumption is that when chitin is located on the exterior of the fungal hyphae, as could be the case for many non-pathogens (e.g. saprotrophs and mycorrhizal symbionts), increased transcript levels of host defense genes are observed at a very early stage in the interaction. For unknown reasons, defence reactions are eventually attenuated during prolonged incubation in the presence of non-pathogenic fungi. Conversely, for many evolutionarily ancient pathogens, where the chitin layer is covered or protected by proteins or glucans (Asiegbu et al. 1999b), a delay in host response could be the norm. Chitin, the basic constituent of fungal cell walls, is targeted by plant chitinases which can degrade the cell wall and actively inhibit the growth of fungi during pathogenic interaction (Boller 1987; Collinge et al. 1993). Chitinases also generate signal molecules that elicit host defence reactions (Kasprzewska 2003). In the ectomycorrhiza associations they may function to degrade chitin fragments, released from the walls of the symbiotic fungus, that would otherwise elicit plant defence responses (Salzer et al. 1997a; Salzer et al. 1997b). Different classes of chitinases with varying specificity are involved in mycorrhiza formation, nodulation and pathogen infection but also plant development (Kasprzewska 2003; Salzer et al. 2000). Both genes coding for chitinases present on the array were differentially expressed in our study during pathogenic and mutualistic interaction (See Supplementary material, Table S2) suggesting that chitin and chitinases may have contributed to the differences observed between global expression profiles of pine challenged with pathogenic or non-pathogenic microorganisms. However, the exact role of chitin and chitinases merits further investigation.

The microarray profiling of *P. sylvestris* response to infection by the fungal pathogen *H. annosum* revealed multiple overlapping strategies employed for defence purposes. Production of pathogenesis-related enzymes and antimicrobial proteins (chitinase, thaumatin, antimicrobial peptide) was supplemented by a

major shift in primary and secondary metabolism (Fig. 3 and 4). A wide array of oxidative stress protecting mechanisms was documented, possibly related to programmed cell death. In turn, analysis of transcript profiling of *P. sylvestris* roots challenged with ectomycorrhizal fungus *L. bicolor* showed transient expression of defence related genes accompanied by shifts in expression of genes with functions related to metabolism, protein fate and transcription (Fig. 3 and 4). A weak or transient induction of defence in response to mutualistic colonisation has been documented in several studies (Barker et al. 1998). One of the genes up-regulated by pine roots in response to both the pathogen and the ectomycorrhizal fungus coded for peroxidase. Peroxidases have been associated with plant defence and resistance, particularly with lignin and suberin synthesis, but also with cross-linking phenolic compounds into papillae and production of toxic compounds (Fossdal et al. 2003) and have also been shown to be transiently up-regulated in the mycorrhizal associations (Blilou et al. 2000; Munzenberger et al. 1997; Spanu and Bonfantefasolo 1988).

In spite of their suggested common evolutionary origin (Hibbett et al. 2000), the saprotrophic and ectomycorrhizal symbiotic interactions investigated in our study displayed very little overlap in terms of differential gene expression (Table 4). Furthermore, there were only four genes regulated in the same way after challenge with the pathogen or the saprotroph; interestingly, two of them had defence-related functions. Although there was a general lack of cellular interaction between the saprotroph and the root, the plant was able to recognise presence of *T. aureoviride*, mount some defence reaction, presumably as a preventive measure, and then largely ignore the fungus.

The existence of a common pattern of response to microbial colonisation was suggested by Güimil et al. (2005). There are genes in legumes that affect symbiosis with both eukaryotic arbuscular mycorrhiza (AM) and prokaryotic *Rhizobia* indicating conservation of symbiotic mechanisms (Ane et al. 2004; Levy et al. 2004). Strikingly, *Rhizobia* and root knot nematodes invoke similar morphological effects in *Lotus japonicus* and elicit common signal transduction events, indicating recruitment of symbiotic pathways by the pathogens (Weerasinghe et al. 2005). Güimil et al. (2005) showed a significant overlap (43%) between AM-specific rice genes and those responding to infection with fungal pathogens. The much smaller overlap observed in our study between the pathogen and mycorrhiza treatment (Table 4), may stem from differences between the hosts (*L. japonicus*, rice, pine), kind of pathogen investigated (nematode, necrotrophic fungus) or symbiotic strategies of ECM and AM fungi. ECM fungi penetrate the host intercellularly and form an extracellular mantle, only transient induction of defence-related genes is observed. On the other hand, AM establish intracellular arbuscules, but in contrast to necrotrophic pathogenic invasion they do not breach the plasmalemma. In addition, the results of our study do not fully reflect mycorrhiza-specific pine response, as at 15 d.p.i. the symbiosis was not fully established and a later time point would be necessary for a full comparison of ectomycorrhizal symbiosis- and pathogenesis-related genes.

However, the existence of a common pattern of response to fungal colonisation is supported by the results of real-time RT-PCR analysis of antimicrobial peptide

expression (Supplementary figure S2). AMP was induced at 1 d.p.i. in all three interactions (although the up-regulation detected by the array in the mycorrhiza interaction had a fold change below the defined threshold). While the up-regulation continued in the roots infected with the pathogen at 5 and 15 d.p.i., in both non-pathogenic systems the expression level was considerably lower. Antimicrobial peptides have been detected in a wide variety of agricultural plant species and have been implicated in resistance of such plants to microbial infections (Broekaert et al. 1997). Apparently, pine AMP represents a broad defence mechanism which might be employed against a wide range of organisms and activated even before recognition mechanisms identify the nature of the microorganism as beneficial, neutral or harmful. However, considering the different trophic strategies and distant taxonomic relation of the three fungal species used in this study, the small overlap detected between plant responses to the microbes is not surprising. Instead, the results suggest that there are specific regulatory patterns of transcriptional responses of conifer trees to colonisation by either mutualists, saprotrophs or pathogens. The genes specific for only one kind of the interaction may be vital for mutualism or disease resistance as opposed to the responses that were shared between pathogen, saprotroph or mutualist that could possibly play a role in compatibility.

Technically, the microarray proved to be a powerful method to elucidate host responses to three different types of fungal interaction. Reproducibility of the hybridization efficiency was confirmed by fold change values exhibited by ESTs belonging to the same contig (Table 2). Real-time RT-PCR verified differential expression of selected genes, although the documented fold changes were generally higher than on the array. Systematic bias of the microarray technique has been reported previously (Yuen et al. 2002). In addition, there is a threshold that defines a minimum sample concentration that must be applied in a given experiment which rendered amplification of RNA isolated from the plant material necessary. SMART™ PCR is a highly efficient method for exponentially amplifying RNA but the nonlinear amplification results in a target in which sequence representation is slightly skewed compared with the original mRNA pool (Puskas et al. 2002; Wadenback et al. 2005). This could have enlarged the differences between the fold changes detected in transcript levels by the microarray and those revealed by real-time RT-PCR. However, other authors have shown that the amplified material faithfully represents the starting mRNA population (Petalidis et al. 2003; Seth et al. 2003). It should also be noted that RNA amplification increases the sensitivity of microarray experiments considerably, allowing the identification of differentially expressed transcripts below the level of detection using targets prepared by direct labelling (Petalidis et al. 2003). Furthermore, with stringent statistical methodology (Wolfinger et al. 2001) and a high number of data points for each gene (36-72), fold change values as low as 1.2 were found to be statistically significant in this study. Moreover, fold changes equal 1.2 as indicated by the array were shown with real-time RT-PCR to correspond to higher values, ranging from 2.1 to 2.9 (Table 3).

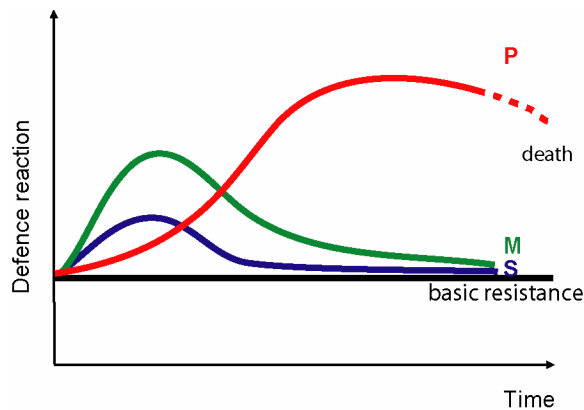


Fig. 6. A model illustrating the observed time-dependent changes in pine response to challenge with a pathogen (P), an ectomycorrhizal symbiont (M) or a saprotroph (S). The saprotroph provokes very weak reaction that declines when it is recognised as neutral microorganism. The ectomycorrhizal fungus induces transient expression of defence-related genes that diminishes over time. On the other hand, the induction of defence in response to the pathogen invasion is initially delayed and increases rapidly with prolonged infection.

Ultimately, a model illustrating the pine response mechanisms in the three different interactions is presented in figure 6. The saprotroph, as an example of an organism not interacting directly with the tree, caused only very little change in gene expression, with an initial peak symbolizing recognition of the presence of the fungus. *Laccaria bicolor*, representing an ectomycorrhizal symbiont, triggered a striking initial response and induction of defence related genes that subsequently declined. The response and induction of defence against the pathogen was delayed and the magnitude increased over time. One interesting feature of our hypothetical model is not whether there are unique genes representing each interaction but rather the magnitude of the gene regulation. Such varying levels of gene expression were particularly noticeable with several defence-related genes. Transient expression was observed with saprotrophic and mycorrhiza fungi during early stages of interaction. On the other hand, a sustainable higher level of induction was documented during pathogenic interaction during prolonged periods of incubation. This has led us to reason that pathogen, saprotroph, or mutualist associated specific molecular patterns may have much to do with gene expression levels and separation in time rather than the absolute uniqueness of the individual genes that are differentially regulated by the host.

In summary, by using a microarray approach, we profiled a diverse range of *P. sylvestris* genes expressed during interaction with either a pathogenic, saprotrophic or mutualistic fungal species. The results indicate that pine was able to recognize all three organisms and specifically distinguish whether they were pathogenic, neutral or beneficial microbial agents.

Acknowledgements

This work was supported by grants from the Swedish Research Council for Environment, Agricultural Sciences and Spatial Planning (FORMAS), the Swedish Science Research Council (VR), Carl Tryggers Stiftelse (CTS), Svenska Cellulosa Aktiebolaget (SCA) and by the Swedish Organization for International Co-operation in Research and Higher Education (STINT).

References

- Ane JM, Kiss GB, Riely BK, Penmetza RV, Oldroyd GED, Ayax C, Levy J, Debelle F, Baek JM, Kalo P, Rosenberg C, Roe BA, Long SR, Denarie J, Cook DR (2004) *Medicago truncatula* DMII required for bacterial and fungal symbioses in legumes. *Science* 303: 1364-1367
- Asiegbu FO, Adomas A, Stenlid J (2005) Conifer root and butt rot caused by *Heterobasidion annosum* (Fr.) Bref. s.l. *Molecular Plant Pathology* 6: 395-409
- Asiegbu FO, Daniel G, Johansson M (1994) Defense related reactions of seedling roots of Norway spruce to infection by *Heterobasidion annosum* (Fr.) Bref. *Physiological and Molecular Plant Pathology* 45: 1-19
- Asiegbu FO, Johansson M, Stenlid J (1999a) Reactions of *Pinus sylvestris* (Scots pine) root tissues to the presence of mutualistic, saprotrophic and necrotrophic micro-organisms. *Journal of Phytopathology-Phytopathologische Zeitschrift* 147: 257-264
- Asiegbu FO, Kacprzak M, Daniel G, Johansson M, Stenlid J, Manka M (1999b) Biochemical interactions of conifer seedling roots with *Fusarium* spp. *Canadian Journal of Microbiology* 45: 923-935
- Barker SJ, Tagu D, Delp G (1998) Regulation of root and fungal morphogenesis in mycorrhizal symbioses. *Plant Physiology* 116: 1201-1207
- Bar-Or C, Kapulnik Y, Koltai H (2005) A broad characterization of the transcriptional profile of the compatible tomato response to the plant parasitic root knot nematode *Meloidogyne javanica*. *European Journal of Plant Pathology* 111: 181-192
- Bilou I, Bueno P, Ocampo JA, Garcia-Garrido J (2000) Induction of catalase and ascorbate peroxidase activities in tobacco roots inoculated with the arbuscular mycorrhizal *Glomus mosseae*. *Mycological Research* 104: 722-725
- Boddy L (1999) Saprotrophic cord-forming fungi: meeting the challenge of heterogeneous environments. *Mycologia* 91: 13-32
- Boller T (1987) Hydrolytic enzymes in plant disease resistance. In: Kosuge T, Nester E (ed) *Plant-Microbe Interactions*. Macmillan, New York, pp 385-413
- Brinker M, van Zyl L, Liu WB, Craig D, Sederoff RR, Clapham DH, von Arnold S (2004) Microarray analyses of gene expression during adventitious root development in *Pinus contorta*. *Plant Physiology* 135: 1526-1539
- Broekaert WF, Cammue BPA, DeBolle MFC, Thevissen K, DeSamblanx GW, Osborn RW (1997) Antimicrobial peptides from plants. *Critical Reviews in Plant Sciences* 16: 297-323
- Campbell GRO, Reuhs BL, Walker GC (2002) Chronic intracellular infection of alfalfa nodules by *Sinorhizobium meliloti* requires correct lipopolysaccharide core. *Proceedings of the National Academy of Sciences of the United States of America* 99: 3938-3943
- Chang S, Puryear J, Cairney J (1993) A simple and efficient method for isolating RNA from pine trees. *Plant Molecular Biology Reporter* 11: 113-116
- Collinge DB, Kragh KM, Mikkelsen JD, Nielsen KK, Rasmussen U, Vad K (1993) Plant chitinases. *Plant Journal* 3: 31-40
- Dixon RA, Lamb CJ (1990) Molecular communication in interactions between plants and microbial pathogens. *Annual Review of Plant Physiology and Plant Molecular Biology* 41: 339-367

- Duchesne LC, Peterson RL, Ellis BE (1987) The accumulation of plant-produced antimicrobial compounds in response to ectomycorrhizal fungi - a review. *Phytoprotection* 68: 17-27
- Dunlap J, Minami E, Bhagwat AA, Keister DL, Stacey G (1996) Nodule development induced by mutants of *Bradyrhizobium japonicum* defective in cyclic B-glucan synthesis. *Molecular Plant-Microbe Interactions* 9: 546-555
- Fossdal CG, Sharma P, Lonneborg A (2003) Isolation of the first putative peroxidase cDNA from a conifer and the local and systemic accumulation of related proteins upon pathogen infection. *Plant Molecular Biology* 47: 423-435
- Fowler S, Thomashow MF (2002) Arabidopsis transcriptome profiling indicates that multiple regulatory pathways are activated during cold acclimation in addition to the CBF cold response pathway. *Plant Cell* 14: 1675-1690
- Galli U, Schuepp H, Brunold C (1994) Heavy-metal binding by mycorrhizal fungi. *Physiologia Plantarum* 92: 364-368
- Greenberg J (1996) Programmed cell death: A way of life for plants. *Proceedings of the National Academy of Sciences of the United States of America* 93: 12094-12097
- Greenberg J (1997) Programmed cell death in plant-pathogen interactions. *Annual Review of Plant Physiology and Plant Molecular Biology* 48: 525-45
- Gu RS, Fonseca S, Puskas LG, Hackler L, Zvara A, Dudits D, Pais MS (2004) Transcript identification and profiling during salt stress and recovery of *Populus euphratica*. *Tree Physiology* 24: 265-276
- Guimil S, Chang HS, Zhu T, Sesma A, Osbourn A, Roux C, Ionnidis V, Oakeley EJ, Docquier M, Descombes P, Briggs SP, Paszkowski U (2005) Comparative transcriptomics of rice reveals an ancient pattern of response to microbial colonization. *Proceedings of the National Academy of Sciences of the United States of America* 102: 8066-8070
- Hahlbrock K, Bednarek P, Ciolkowski I, Hamberger B, Heise A, Liedgens H, Logemann E, Nurnberger T, Schmelzer E, Somssich IE, Tan JW (2003) Non-self recognition, transcriptional reprogramming, and secondary metabolite accumulation during plant/pathogen interactions. *Proceedings of the National Academy of Sciences of the United States of America* 100: 14569-14576
- Hashimoto JG, Beadles-Bohling AS, Wren KM (2004) Comparison of RiboGreen (R) and 18S rRNA quantitation for normalizing real-time RT-PCR expression analysis. *Biotechniques* 36: 54-60
- Henry CM, Deacon JW (1981) Natural non-pathogenic death of the cortex of wheat and barley seminal roots as evidenced by nuclear stain with acridine orange. *Plant and Soil* 60: 255-274
- Hibbett DS, Gilbert LB, Donoghue MJ (2000) Evolutionary instability of ectomycorrhizal symbioses in basidiomycetes. *Nature* 407: 506-508
- Jin W, Riley RM, Wolfinger RD, White KP, Passador-Gurgel G, Gibson G (2001) The contributions of sex, genotype and age to transcriptional variance in *Drosophila melanogaster*. *Nature Genetics* 29: 389-395
- Johansson T, Le Quere A, Ahren D, Soderstrom B, Erlandsson R, Lundeberg J, Uhlen M, Tunlid A (2004) Transcriptional responses of *Paxillus involutus* and *Betula pendula* during formation of ectomycorrhizal root tissue. *Molecular Plant-Microbe Interactions* 17: 202-215
- Jones DA, Takemoto D (2004) Plant innate immunity - direct and indirect recognition of general and specific pathogen-associated molecules. *Current Opinion in Immunology* 16: 48-62
- Kasprzewska A (2003) Plant chitinases-regulation and function. *Cellular and Molecular Biology Letters* 8: 809-824
- Kawasaki S, Borchert C, Deyholos M, Wang H, Brazille S, Kawai K, Galbraith D, Bohnert HJ (2001) Gene expression profiles during the initial phase of salt stress in rice. *Plant Cell* 13: 889-905
- Kirst M, Johnson AF, Baucom C, Ulrich E, Hubbard K, Staggs R, Paule C, Retzel E, Whetten R, Sederoff R (2003) Apparent homology of expressed genes from wood-

- forming tissues of loblolly pine (*Pinus taeda* L.) with *Arabidopsis thaliana*. Proceedings of the National Academy of Sciences of the United States of America 100: 7383-7388
- Levy J, Bres C, Geurts R, Chalhoub B, Kulikova O, Duc G, Journet EP, Ane JM, Lauber E, Bisseling T, Denarie J, Rosenberg C, Debelle F (2004) A putative Ca²⁺ and calmodulin-dependent protein kinase required for bacterial and fungal symbioses. Science 303: 1361-1364
- Manthey K, Krajinski F, Hohnjec N, Firnhaber C, Puhler A, Perlick AM, Kuster H (2004) Transcriptome profiling in root nodules and arbuscular mycorrhiza identifies a collection of novel genes induced during *Medicago truncatula* root endosymbioses. Molecular Plant-Microbe Interactions 17: 1063-1077
- Martin F, Tuskan GA, DiFazio SP, Lammers P, Newcombe G, Podila GK (2004) Symbiotic sequencing for the *Populus mesocosm*. New Phytologist 161: 330-335
- Mazau D, Rumeau D, Esquerretugaye MT (1987) Molecular approaches to understanding cell-surface interactions between plants and fungal pathogens. Plant Physiology and Biochemistry 25: 337-343
- McFadden HG, Wilson IW, Chapple RM, Dowd C (2006) Fusarium wilt (*Fusarium oxysporum* f. sp. *vasinfectum*) genes expressed during infection of cotton (*Gossypium hirsutum*). Molecular Plant Pathology 7: 87-101
- Mithofer A (2002) Suppression of plant defence in rhizobia-legume symbiosis. Trends in Plant Science 7: 440-444
- Mohr U, Lange J, Boller T, Wiemken A, Vogeli-Lange R (1998) Plant defence genes are induced in the pathogenic interaction between bean roots and *Fusarium solani*, but not in the symbiotic interaction with the arbuscular mycorrhizal fungus *Glomus mosseae*. New Phytologist 138: 589-598
- Munzenberger B, Otter T, Wustrich D, Polle A (1997) Peroxidase and laccase activities in mycorrhizal and non-mycorrhizal fine roots of Norway spruce (*Picea abies*) and larch (*Larix decidua*). Canadian Journal of Botany-Revue Canadienne De Botanique 75: 932-938
- Ozturk ZN, Talame V, Deyholos M, Michalowski CB, Galbraith DW, Gozukirmizi N, Tuberosa R, Bohnert HJ (2002) Monitoring large-scale changes in transcript abundance in drought- and salt-stressed barley. Plant Molecular Biology 48: 551-573
- Pearce RB (1996) Antimicrobial defences in the wood of living trees. New Phytologist 132: 203-233
- Petalidis L, Bhattacharyya S, Morris GA, Collins VP, Freeman TC, Lyons PA (2003) Global amplification of mRNA by template-switching PCR: linearity and application to microarray analysis. Nucleic Acids Research 31:
- Puskas LG, Zvara A, Hackler L, Van Hummelen P (2002) RNA amplification results in reproducible microarray data with slight ratio bias. Biotechniques 32: 1330-1340
- Salzer P, Bonanomi A, Beyer K, Vogeli-Lange R, Aeschbacher RA, Lange J, Wiemken A, Kim D, Cook DR, Boller T (2000) Differential expression of eight chitinase genes in *Medicago truncatula* roots during mycorrhiza formation, nodulation, and pathogen infection. Molecular Plant-Microbe Interactions 13: 763-777
- Salzer P, Hebe G, Hager A (1997a) Cleavage of chitinous elicitors from the ectomycorrhizal fungus *Hebeloma crustuliniforme* by host chitinases prevents induction of K⁺ and Cl⁻ release, extracellular alkalization and H₂O₂ synthesis of *Picea abies* cells. Planta 203: 470-479
- Salzer P, Hubner B, Sirrenberg A, Hager A (1997b) Differential effect of purified spruce chitinases and beta-1,3-glucanases on the activity of elicitors from ectomycorrhizal fungi. Plant Physiology 114: 957-968
- Seki M, Narusaka M, Ishida J, Nanjo T, Fujita M, Oono Y, Kamiya A, Nakajima M, Enju A, Sakurai T, Satou M, Akiyama K, Taji T, Yamaguchi-Shinozaki K, Carninci P, Kawai J, Hayashizaki Y, Shinozaki K (2002) Monitoring the expression profiles of 7000 Arabidopsis genes under drought, cold and high-salinity stresses using a full-length cDNA microarray. Plant Journal 31: 279-292
- Seth D, Gorrell MD, McGuinness PH, Leo MA, Lieber CS, McCaughan GW, Haber PS (2003) SMART amplification maintains representation of relative gene expression:

- quantitative validation by real time PCR and application to studies of alcoholic liver disease in primates. *Journal of Biochemical and Biophysical Methods* 55: 53-66
- Silberbach M, Huser A, Kalinowski J, Puhler A, Walter B, Kramer R, Burkovski A (2005) DNA microarray analysis of the nitrogen starvation response of *Corynebacterium glutamicum*. *Journal of Biotechnology* 119: 357-367
- Smith CM, Rodriguez-Buey M, Karlsson J, Campbell MM (2004) The response of the poplar transcriptome to wounding and subsequent infection by a viral pathogen. *New Phytologist* 164: 123-136
- Smith S, Read D (1997) Mycorrhizal symbiosis. Academic Press, London
- Smith SE, Gianinazzepearson V, Koide R, Cairney JWG (1994) Nutrient transport in mycorrhizas - structure, physiology and consequences for efficiency of the symbiosis. *Plant and Soil* 159: 103-113
- Spanu P, Bonfantefasolo P (1988) Cell-wall-bound peroxidase-activity in roots of mycorrhizal *Allium porrum*. *New Phytologist* 109: 119-124
- Stasolla C, Bozhkov PV, Chu TM, Van Zyl L, Egertsdotter U, Suarez MF, Craig D, Wolfinger RD, Von Arnold S, Sederoff RR (2004) Variation and transcript abundance during somatic embryogenesis in gymnosperms. *Tree Physiology* 24: 1073-1085
- Stasolla C, van Zyl L, Egertsdotter U, Craig D, Liu WB, Sederoff RR (2003) The effects of polyethylene glycol on gene expression of developing white spruce somatic embryos. *Plant Physiology* 131: 49-60
- Stenlid J (1985) Population structure of *Heterobasidion annosum* as determined by somatic incompatibility, sexual incompatibility and isozyme patterns. *Canadian Journal of Botany* 63: 2268-2273
- Tagu D, Martin F (1996) Molecular analysis of cell wall proteins expressed during the early steps of ectomycorrhiza development. *New Phytologist* 133: 73-85
- Tagu D, Python M, Cretin C, Martin F (1993) Cloning symbiosis-related cDNAs from Eucalypt ectomycorrhiza by PCR-assisted differential screening. *New Phytologist* 125: 339-343
- van Zyl L, von Arnold S, Bozhkov P, Chen YZ, Egertsdotter U, MacKay J, Sederoff RR, Shen J, Zelena L, Clapham DH (2002) Heterologous array analysis in Pinaceae: hybridization of *Pinus taeda* cDNA arrays with cDNA from needles and embryogenic cultures of *P. taeda*, *P. sylvestris* or *Picea abies*. *Comparative and Functional Genomics* 3: 306-318
- Vasiliauskas R, Menkis A, Finlay RD, Stenlid J (2007) Wood-decay fungi in fine living roots of conifer seedlings. *New Phytologist* in press, doi: 10.1111/j.1469-8137.2007.02014.x:
- Wadenback J, Clapham DH, Craig D, Sederoff R, Peter GF, von Arnold S, Egertsdotter U (2005) Comparison of standard exponential and linear techniques to amplify small cDNA samples for microarrays. *BMC Genomics* 6:
- Watkinson JI, Sioson AA, Vasquez-Robinet C, Shukla M, Kumar D, Ellis M, Heath LS, Ramakrishnan N, Chevone B, Watson LT, van Zyl L, Egertsdotter U, Sederoff RR, Grene R (2003) Photosynthetic acclimation is reflected in specific patterns of gene expression in drought-stressed loblolly pine. *Plant Physiology* 133: 1702-1716
- Weerasinghe RR, Bird DM, Allen NS (2005) Root-knot nematodes and bacterial Nod factors elicit common signal transduction events in *Lotus japonicus*. *Proceedings of the National Academy of Sciences of the United States of America* 102: 3147-3152
- Wolfinger RD, Gibson G, Wolfinger ED, Bennett L, Hamadeh H, Bushel P, Afshari C, Paules RS (2001) Assessing gene significance from cDNA microarray expression data via mixed models. *Journal of Computational Biology* 8: 625-637
- Yuen T, Wurmbach E, Pfeffer RL, Ebersole BJ, Sealfon SC (2002) Accuracy and calibration of commercial oligonucleotide and custom cDNA microarrays. *Nucleic Acids Research* 30: e48

Tables

Table 1. Adhesion and colonisation of *Pinus sylvestris* root tissues by a saprotroph (*T. aureoviride*), a pathogen (*H. annosum*) or an ectomycorrhiza symbiont (*L. bicolor*) at 1, 5 and 15 d.p.i.

	Saprotroph ^a	Ectoycorrhiza ^b	Pathogen ^c
1 d.p.i.			
Adhesion	x	x	x
Penetration into:			
protodermal cells	-	-	x
epidermal cells	-	-	x
cortex	-	-	-
vascular tissues	-	-	-
5 d.p.i.			
protodermal cells	-	-	x
epidermal cells	-	-	x
cortex	-	-	x
vascular tissues	-	-	-
15 d.p.i.			
protodermal cells	x ^d	x ^d	x
epidermal cells	x ^d	-	x
cortex	-	-	x
vascular tissues	-	-	x

^a this study

^b Heller et al., in preparation

^c Adomas et al., in press

^d Intercellular penetration

Table 2. Functional classification of 41 ESTs differentially expressed by *P. sylvestris* roots challenged with a saprotrophic fungus *T. aureoviride* at 1, 5 or 15 d.p.i. as compared to uninoculated control^a

Contig	CloneID	putative function	1 dpi	5 dpi	15 dpi
Metabolism					
	39 D04	ferredoxin thioredoxin reductase	1.3		
	NXCI_006_A10	laccase			-1.3
	NXNV_164_H08	putative xyloglucan endotransglycosylase			1.3
1	NXPV_088_C08	xyloglucan endo-transglycosylase			1.3
1	NXSI_103_E12	xyloglucan endo-transglycosylase			1.3
	NXSI_113_E06	xyloglucan endo-transglycosylase			1.3
	NXSI_134_F04	endo-beta-1,4-glucanase	-1.2		
Energy					
	07 C06	quinone oxidoreductase	1.3		
Transcription					
	ST 29 G04	zinc finger protein	1.3		
	NXCI_115_E10	nuclear RNA binding protein	-1.3		
	NXNV 044 B12	scarecrow-like 1 (transcription factor)			-1.2
Protein synthesis					
	08 B07	ribosomal protein S27	1.3		
	36 F09	60S ribosomal protein L	1.3		
	38 E02	60S ribosomal protein L	1.3		
Protein fate					
	03 G03	10 kDa chaperonin	1.2		
Transport					
	03 E05	mitochondrial inner membrane translocase		1.3	
	04 A02	oxoglutarate/malate translocator	1.4		
	27 D10	protein transporter	1.3		
3	19 E08	non specific lipid transfer protein precursor			-1.3
3	NXSI_089_H07	nonspecific lipid-transfer protein precursor			-1.4
Communication and signalling					
	NXSI_030_C06	calcium binding protein			1.4
Cell rescue and defence					
	04 G06	antimicrobial peptide	1.3		
	33 E05	immunophilin	1.2		
	NXSI_064_A03	thaumatin	1.3		
	NXSI_012_D08	peroxidase	1.2		
	27 G09	metallothionein			-1.2
Development					
	ST 32 C09	putative late embryogenesis abundant	1.2		

	Control of cellular organization		
	20 A07	histone H3	1.2
	40 E09	histone H3	1.2
	Unknown		
	NXCI_115_E10	no hit	-1.3
	04 E06	unknown	1.4
	11 D07	unknown	1.3
2	12 G02	unknown	1.3
	18 H01	no hit	1.3
	33 D01	unknown	1.2
	38 F09	unknown	1.3
	NXCI_036_H12	no hit	1.3
	NXSI_054_F05	glycine-rich protein	1.3
2	NXSI_109_B12	hypothetical protein	1.3
	NXSI_122_A12	no hit	1.3
	34 E10	no hit	-1.2
	37 H11	unknown	-1.3
	NXCI_029_F09	unknown	-1.3

^a The ESTs were determined by the microarray to be differentially expressed if the fold change was ≥ 1.2 or ≤ -1.2 . The ESTs forming contigs were marked with numbers 1-3. Some of the ESTs could have been prescribed to more than one functional group

Table 3. Fold changes of selected gene transcripts determined by real-time RT-PCR in *P. sylvestris* root tissues challenged with *T. aureoviride* at 1, 5 or 15 d.p.i. as compared to uninoculated control ^a

Gene ID	Putative function	Array	Real-time RT-PCR ^b		
1 d.p.i.					
ST29G04	zinc finger protein	1.3	1.6	±	0.2
ST 04 G06	antimicrobial peptide	1.3	4.3	±	1.2
NXSI_012_D08	peroxidase	1.2	2.1	±	0.6
NXSI_134_F04	endo-beta-1,4 glucanase	-1.2	-18.0	±	22.4
5 d.p.i.					
ST20A07	histone H3	1.2	2.9	±	0.7
15 d.p.i.					
NXNV_164_H08	xyloglucan endotransglycosylase	1.3	14.2	±	9.2

^a Distribution of number of copies of biological replicates is presented in Supplementary materials Fig. S1a-f

^b Fold changes determined by real-time RT-PCR ± standard deviation.

Table 4. Number of genes differentially expressed by *P. sylvestris* roots challenged with a pathogenic (*H. annosum*) [P], ectomycorrhiza (*L. bicolor*) [M] or a saprotrophic fungus (*T. aureoviride*) [S] and genes commonly regulated in different treatments (PM, PS, MS and PMS) at 1, 5 or 15 d.p.i. as compared to un-infected control. The numbers in brackets correspond to number of genes up- and down, regulated respectively. ^a

Time	P	M	S	PMS	PM	PS	MS
1 d.p.i.	17 (7, 10)	284 (161, 123)	27 (23, 4)	0	9 (3, 6)	2 (2, 0)	3 (0, 3)
5 d.p.i.	67 (50, 18)	60 (53, 6)	2 (2, 0)	0	2 (1, 1)	0 (0, 0)	0 (0, 0)
15 d.p.i.	277 (176, 100)	20 (12, 8)	12 (6, 6)	0	14 (9, 5)	2 (0, 2)	2 (2, 0)

^a The ESTs were determined by the microarray to be differentially expressed if the fold change was ≥ 1.2 or ≤ -1.2

Supplementary materials

The data discussed in this publication have also been deposited at NCBI Gene Expression Omnibus (GEO, <http://www.ncbi.nlm.nih.gov/geo/>) and are accessible through GEO platform GPL4039, series accession numbers: GSE5407, GSE5408 and GSE5410. The following supplementary material accompanies the manuscript:

Table S1. Primers used for the real-time RT-PCR experiment.

Gene ID	Putative function	Primer sequences	
		Forward	Reverse
ST29G04	zinc finger protein	GTGGCCTTCGGAATGATTTA	ATGAGGTTTTGGCAGTGTCC
ST 04 G06	antimicrobial peptide	AATGTGGGTGTTCTAATATCGGCA	AAGCTTTATTTGGGACAACGCC
NXSI_012_D08	peroxidase	TGAAGGAGTTTGCCTGAAT	AGCTGGCTCATCTTCACCAT
NXSI_134_F04	endo-beta-1,4 glucanase	ATCAATGCTCCTTTGGTTGG	GCGAAACTGTGTGCCAAATA
ST20A07	histone H3	GCACGGAGCTTTTGATAAGG	GCAGAGGACTGGAACCTCAG
NXNV_164_H08	xyloglucan endotransglycosylase	TATCCCCAACAACGAGAGG	TACCCTCATGGGCTGTTTCT

Table S2. Genes differentially expressed by *P. sylvestris* roots in response to challenge with *L. bicolor* (M), *H. annosum* (P) or *T. aureoviride* (S) at 1, 5 or 15 d.p.i .

Gene ID	Putative function	1	1	1	5	5	5	15	15	15	Cluster	
		dpi M	dpi P	dpi S	dpi M	dpi P	dpi S	dpi M	dpi P	dpi S		
01_F04	elongation factor 1-ALPHA				-1.2						4	9
01_G02	GASA5-like protein								1.3		11	16
02_A06	hypothetical protein								1.2			16
02_B03	probable cinnamyl-alcohol dehydrogenase					1.6			2.4		12	19
02_C01	protease regulatory subunit 7	-1.2									4	
02_C09	antifreeze-like protein (AF70)				1.3						4	10
02_D01	protein kinase PK1	-1.3									5	
02_E09	aconitate hydratase, cytoplasmic						1.3				4	12
02_F09	histone-like protein	-1.5									5	
03_B07	intracellular pathogenesis related protein PINMIII								1.3			16
03_C08	chlorophyll a/b binding protein CP29 precursor				1.4				-1.3		1	10 17
03_C11	ubiquitin precursor				1.3						4	10
03_D08	Pollen allergen Che a 1 precursor	-1.3									5	15
03_E05	protein translocase	-1.3					1.3				4	15
03_F07	no hit	1.3	1.3						1.3		3	16
03_G03	10 kda chaperonin			1.2							2	
04_A02	oxoglutarate/malate translocator			1.4							2	
04_B03	no hits found	-1.3									4	
04_C10	chitinase	-1.3					-1.3				5	8
04_D07	cyclophilin	-1.2									4	
04_D11	unknown						-1.2				2	11 17
04_E06	unknown			1.4							2	
04_E10	unknown								1.3		6	16

04_F01	unknown					1.3		19
04_G06	antimicrobial peptide	1.6	1.3				6	
05_H03	putativeWD-40 repeat protein, MSI4					1.3	1	16
06_A10	NADH dehydrogenase subunit 2					1.3	1	16
06_E01	histone H3 - wheat	1.4	1.3				3	
06_F05	putative beta-ketoacyl-CoA synthase					1.3		18
06_G07	ATP-dependent CLP protease subunit CLPP					1.3	1	16
06_H04	unknown	-1.3					5	20
06_H09	glycolate oxidase	-1.3		-1.3			7	11
07_A03	aquaporin				-1.3	-2.1		17
07_A05	no hit					-1.4	3	15
07_A07	hyp pro	-1.3					4	
07_C06	quinone oxidoreductase			1.3			2	
07_D02	probable purine NTPase PAB0812	1.3					3	
07_E10	unknown	1.4	1.4				6	15
07_E12	unknown	1.3					1	18
07_F08	ubiquitin conjugating enzyme - tomato	-1.3					4	
07_F10	actin depolymerizing	-1.3					4	
07_F11	hypothetical protein					-1.5	2	17
08_B05	tubulin alpha-2/alpha-	-1.3					4	
08_B07	ribosomal protein S27			1.3			2	
08_H06	metallothionein-like protein EMB30					1.3	3	16
09_F02	20S proteasome subunit PAF1	-1.3					7	
11_D05	unknown					1.4		12
11_D07	unknown		1.3				2	18
12_A02	unknown			1.4			4	10
12_A08	unknown					-1.3	2	17
12_B10	putative t-complex pro/ATP binding/protein binding	1.3				1.4	1	16
12_D01	photosystem i reaction center subunit					-1.6		11
12_G02	unknown		1.3				2	17

13_C11	hypothetical protein	-1.3				7	
13_C12	putative peptidyl-prolyl isomerase	-1.2				5	
13_G11	nucleoside diphosphate	-1.3				2	
13_H06	leucoanthocyanidin dioxygenase				1.4	7	16
14_B06	actin	-1.3	-1.2			4	8
14_B10	heat shock protein				-1.4	4	17
14_D09	no hit				1.2	1	16
15_B11	translation initiation factor 3-like protein				1.2		18
15_D07	pollen specific protein C13 precursor	-1.3				5	
15_G03	chloroplast 30S ribosomal protein				-1.3		17
15_H06	unknown		1.3			2	10
16_C01	no hit				1.2		19
16_F06	stress responsive protein	-1.3				5	
16_G12	inorganic phosphatase	-1.4				7	
17_A11	DNA binding / RNA binding	-1.3				4	
17_E04	phosphoserine aminotransferase		1.3			4	12
17_G12	putative cytochrome P450 protein				1.3	3	19
17_H11	no hit				1.3	2	16
18_H01	no hit		1.3			2	
18_H08	CER-1 like protein	1.3			1.3	3	18
18_H10	phosphoribolucinase precursor				-1.4	3	15
19_A12	no hit				-1.7	3	17
19_B12	developmental protein	-1.3				4	
19_D12	ribosomal protein s16	-1.2				4	
19_E08	non specific lipid transfer protein precursor	-1.3				-1.3	5
20_A07	histone H3			1.2		2	15
20_C09	glutamine synthase	-1.2				5	
20_D09	succinylhomoserine sulfhydrylase	-1.3				4	
20_H10	reversibly glycosylated polypeptide	-1.3				4	
21_A12	splicing factor rszp-2	-1.3				7	
21_D09	unknown	-1.3				7	

21_E01	FAD binding / aldehyde-lyase/ oxidoreductase/ oxidoreductase, acting on CH-OH group of donors	1.2		1.3	3	16
21_E04	glyceraldehyde-3-phosphate dehydrogenase			1.3		19
21_E12	no hits	-1.3			7	
21_F11	elongation factor 1-A1	-1.3			4	
21_G02	thioredoxin-like protein	-1.3			7	
21_H02	expansin9 precursor	-1.2			4	
22_A06	homeobox proteinPpHB7			1.3	3	18
22_B04	hyp pro	-1.3			5	
22_E07	arginine decarboxylase	-1.4			7	
22_F09	tubulin alpha-1 chain	-1.3			5	
22_F10	endo-xyloglucan transferase (fragment)		1.3		4	15
22_G10	adenosine kinase-like protein	-1.3			4	
23_A08	water stress inducible protein			-1.8		17
23_B10	hypothetical protein			-1.2	2	17
23_C10	catalase (EC1.11.1.6) (fragment)	-1.3			4	
23_F07	ATP-citrate-lyase		1.6	1.9	4	12 19
23_G12	trans-cinnamate 4-monooxygenase		1.6	2.2	6	12 19
24_B06	stress related protein	-1.2			4	
24_C06	5-methyltetrahydropteroyltriglutamate (methionine synthase)	-1.3		1.5	4	19
24_D05	hypothetical protein	-1.3			5	
24_F06	unknown	-1.3	-1.2		7	
24_G05	no hit			1.4	6	12
25_B04	actin 1	-1.2			5	
25_C10	hypothetical	1.4			3	
25_C11	putative retroelement pol polyprotein	-1.4			5	
26_A12	no hits			1.2	1	19
26_D05	ATP synthase c-chain			-1.5	6	17
27_A08	no hit	-1.3			4	

27_D07	enoyl-CoA-hydratase		1.3			3	10	
27_D10	protein transporter		1.3			2		
27_G09	metallothionein				-1.4	-1.2	7	20
28_A11	alcohol dehydrogenase				1.3		12	19
28_A12	Ribosomal protein S3A	1.3					1	
28_B11	Narenginin-2-oxoglutarate-3-dioxygenase	-1.2					4	
28_C03	unknown	-1.2					4	
28_F04	no hit	-1.3					5	
28_G07	Ran binding protein		1.4					10
29_E10	RNA binding / nucleic acid binding	-1.3					4	
29_G11	no hit	-1.3					5	
30_A12	ubiquitin-specific protease	-1.3					5	17
31_D06	glutathione transferase (EC 2.5.1.18)			1.5			4	12
32_B09	celldivision cycle protein 48 homologous	-1.3					5	
32_D11	hypothetical protein	-1.3					5	
32_E12	hypothetical protein	-1.3					7	
32_F07	hypothetical protein					1.4	6	16
32_G03	no hit					1.6	5	16
33_A12	40S ribosomal protein like				1.3	1.3		18
33_D01	unknown		1.2				2	
33_E05	immunophilin		1.2				2	
33_E11	phosphate transporter	-1.4					7	
33_F10	hypothetical protein	-1.2					2	
33_H11	no hit					1.3	3	16
34_B04	GASA5-like protien					1.4		16
34_E10	no hit	-1.3	-1.2				5	
34_F04	putative cinnamoyl CoA reductase					1.8		16
35_G10	WD-40 repeat protein	-1.3					4	
35_H05	hypothetical protein	-1.3					5	
36_A10	chlorophyll a/b binding pro					-1.9	6	11
36_B02	plastid protein	-1.3					5	17

36_F09	60S ribosomal protein L									2	
37_B10	hypothetical protein	-1.2								4	
37_E10	gibberellin regulated protein	-1.3	-1.2		-1.2	-1.6				7	8
37_H02	LTP family protein								1.3		16
37_H11	unknown	-1.3			-1.3				1.2	5	19
38_B07	membrane intrinsic protein Mip-2	-1.3								5	
38_C01	hypothetical protein	-1.3								7	
38_E02	60S ribosomal protein L									2	
38_F09	unknown									2	
39_B12	RUBISCO subunit binding protein alpha subunit	-1.3								4	
39_C06	hypothetical protein	-1.2								7	
39_D04	ferredoxin thioredoxin reductase									2	18
40_A03	porine MIP1	-1.4								5	17
40_D10	S-adenosylmethionine synthetase										12
40_E08	cystein proteinase inhibitor BCPA2	-1.3								4	
40_E09	histone H3									2	11
40_H09	calmodulin	1.3								3	
NXCI_001_A06	beta tubulin	-1.4								7	
NXCI_002_B01	(1-4)-beta-mannan endohydrolase									1.3	16
NXCI_002_C10	putative dehydrin	1.3								1	
NXCI_002_E07	leucoanthocyanidin reductase									1.9	19
NXCI_002_G06	Blast for putative function	1.3								1	
NXCI_002_H04	H+ transporting ATP synthase (EC 3.6.1.34)	1.3								1	
NXCI_005_B11	TIR/P-loop/LRR									-1.8	17
NXCI_005_C10	laccase (EC 1.10.3.2)	1.3								1.3	16
NXCI_005_G03	purple acid phosphatase	1.3								1.4	10
NXCI_006_A10	laccase									1.2	-1.3
NXCI_006_F01	ubiquinol-cytochrome C reductase	1.3								1	
NXCI_008_C01	photosystem ii oxygen-evolving complex protein	1.3								-1.9	11
NXCI_008_H10	putative zinc-finger protein	1.3								1	8
											20

NXCI_009_A10	no hit	1.3				1		
NXCI_009_C07	no hit	1.3				1		
NXCI_012_H07	probable transcription factor sf3				-1.4			17
NXCI_017_C07	ferritin 2 precursor - cowpea	1.3				1		16
NXCI_018_A08	pectate lyase	1.4			1.5	1		19
NXCI_018_F10	pinoresinol-lariciresinol reductase	1.3				1		22
NXCI_018_G04	aldehyde dehydrogenase homolog	1.3				1		
NXCI_020_A02	embryonic abundant protein	1.3				1		
NXCI_020_A08	type 2 light-harvesting chlorophyll a/b-binding				-1.4			17
NXCI_021_D03	proline-rich protein	1.3			1.3	1		16
NXCI_021_G04	late embryonic abundant protein		-1.3		-2.0		15	17
NXCI_021_G04	late embryonic abundant protein		-1.3		-1.7		15	17
NXCI_022_B04	no hit	1.3				1		
NXCI_022_E07	no hit	1.3				1	9	
NXCI_022_G01	heat shock 70 kDa protein, mitochondrial	1.4				1		22
NXCI_025_G06	plastid-specific ribosomal protein	1.3				1		
NXCI_026_A11	putative glutaredoxin	1.4				1		
NXCI_026_C06	putative cytochrome B5	1.3				1	8	
NXCI_027_D03	no hit	1.3				1		
NXCI_027_E04	no hit				-1.6	1		17
NXCI_027_E09	allyl alcohol dehydrogenase	1.3				1		
NXCI_029_D03	40S ribosomal protein S15	1.3				1		
NXCI_029_F09	unknown		1.8		2.6	-1.3	3	12
NXCI_031_H08	2,3-bisphosphoglycerate-independent phosphatase		1.3					10
NXCI_032_C05	ferredoxin	1.2				1		
NXCI_032_E01	aspartate carbamoyl transferase	1.3	1.3		1.3	1	10	19
NXCI_032_F09	sucrose synthase	1.2				1		
NXCI_032_F11	lectin - like protein				-1.6			17
NXCI_032_H03	cullin-like protein	1.2				1		
NXCI_034_F04	no hit	1.3				1		

NXCI_036_H12	no hit		1.3		1.3		3		19
NXCI_037_A03	ribosomal protein S15A				1.3		1		19
NXCI_037_B03	hypothetical protein		1.2					14	
NXCI_042_G11	cation-transporting ATPase	1.3					1		18
NXCI_043_D02	Phosphoglycerate dehydrogenase	1.3					1		
NXCI_044_A12	PREG-like protein (fragment)	1.4			-1.3		1		17
NXCI_045_C01	no hit	1.3			1.4		1	11	16
NXCI_045_H07	MLO protein homolog 1	1.4					1		
NXCI_046_E05	laccase (diphenol oxidase)	1.3			3.1		1		19
NXCI_047_C08	transporter-like protein	1.3					1		
NXCI_048_B08	dihydrolipoamide acetyltransferase	1.3					1		
NXCI_048_E08	probable aquaporin	1.2					1		
NXCI_050_B07	s-adenosylmethionine synthetase 3				1.8				19
NXCI_050_C10	no hit				-1.3				17
NXCI_050_F08	40S ribosomal protein	1.4					3		
NXCI_053_F03	adenosylhomocysteinase (EC 3.3.1.1)		-1.3		1.2	1.8		9	16
NXCI_054_C06	GTP-binding protein-like	1.2					1		
NXCI_054_D12	lipid transfer protein	1.3					1		
NXCI_054_E06	similarity to transcription factor	1.3					1		
NXCI_054_H03	probable endopeptidase Clp ATP-binding chain	1.3					1		
NXCI_055_C01	methionine synthase		1.3						12
NXCI_055_D01	putative surface protein, endosperm specific		-1.4		-1.9		1	11	17
NXCI_055_D02	SRG1 protein - anthocyanidin synthase	1.3	1.8		3.4		3	12	19
NXCI_055_D03	metallothionein-like protein	1.3					1	14	
NXCI_056_A03	putative auxin-induced	1.2			1.3		3		16
NXCI_056_C02	spliceosome-associated protein	1.2					1		
NXCI_056_E02	no hit	1.3			1.3		1		19
NXCI_056_E12	elongation factor 1-alpha	1.3					1		
NXCI_057_A08	40S ribosomal protein S17	1.3					1		
NXCI_057_B05	pectate lyase				1.3				19

NXCI_058_C02	histone H4	1.3				1		
NXCI_062_B10	probable gamma-thionin precursor SPII	1.2				1		
NXCI_062_H01	putative auxin-induced	-1.3				7		
NXCI_064_E04	prephenate dehydratase (EC 4.2.1.51)			1.5		2	12	19
NXCI_066_A11	thiamine biosynthetic enzyme 1-2 precursor			-1.7				17
NXCI_066_G08	3-ketoacyl-CoA thiolase B peroxisomal	-1.3				4		
NXCI_066_H04	acetoacyl-CoA-thiolase.		2.1	1.7		6	12	19
NXCI_067_C08	no hit	1.3				1		
NXCI_067_D08	GTP-binding nuclear protein	1.4				1		
NXCI_067_H06	sterol-C-methyltransferase			-1.3				17
NXCI_068_C12	polygalacturonase-like protein	1.2	1.3			3	10	
NXCI_068_D10	COP9 signalosome complex subunit 4		1.4				10	
NXCI_069_A02	no hit			2.3			10	19
NXCI_070_B10	translation initiation factor EIF-1A		1.3			1	10	
NXCI_070_E11	vacuolar proton pyrophosphatase	-1.4				5		
NXCI_075_B02	GTP-binding protein		1.4				10	
NXCI_075_C07	probable NADH-glutamate synthase		1.6	1.2		1	10	
NXCI_075_D09	epoxide hydrolase			1.5				19
NXCI_075_E11	mitochondrial NADH:ubiquinone oxidoreductase			1.9				19
NXCI_082_D08	carbonate dehydratase (EC 4.2.1.1)	-1.3				7		
NXCI_082_E07	xyloglucan endo-transglycosylase			-1.7		5		17
NXCI_082_E07	xyloglucan endo-transglycosylase			-1.9		5		17
NXCI_083_F01	no hit			-1.7				17
NXCI_084_G02	alcohol dehydrogenase (EC 1.1.1.1)		1.2	1.6		1	12	19
NXCI_085_H12	glutathione s-transferase		1.6			4	12	16
NXCI_086_H02	phospho-2-dehydro-3-deoxyheptonate aldolase			-1.3		7		17
NXCI_087_F07	cinnamate-4-hydroxylase		1.4	1.8			12	19
NXCI_093_B07	trans-cinnamate 4-hydroxylase (EC		1.3				10	

	1.14.13.11)						
NXCI_093_E01	protein disulfide isomerase			1.2			16
NXCI_093_F03	abscisic acid water deficit stress and ripening inducible		-1.3	-1.7	1		17
NXCI_093_H05	phenylalanine ammonia-lyase (EC 4.3.1.5)		1.5	2.1		12	19
NXCI_094_B03	carnitine racemase		1.3			10	
NXCI_094_C09	laccase (EC 1.10.3.2)	1.3			1		19
NXCI_094_E12	pectate lyase			1.3			19
NXCI_095_D10	calmodulin-bindin	-1.3			4		
NXCI_096_C10	no hit	1.3			1		
NXCI_097_F03	poly(A)-binding protein	1.3			1		
NXCI_098_D10	cytochrome P450	1.4			3		
NXCI_098_F10	chalcone-flavonone isomerase			1.4			16
NXCI_101_B08	beta-glucosidase.	1.3			1		
NXCI_101_B10	endo-beta-1,4-glucanase	1.3			1		
NXCI_101_C06	cytochrome C oxidase	1.3			1		
NXCI_101_D04	polyphosphoinositide binding protein Ssh2	1.4			1		
NXCI_101_G04	40S ribosomal protein	1.3			1		
NXCI_102_C08	probable mannitol dehydrogenase	1.4			1		
NXCI_102_D01	dehydration-induced protein erd15	1.3			1		
NXCI_102_F06	putative signal sequence receptor	1.3			1		
NXCI_102_G08	60S acidic ribosomal protein	1.3			1		
NXCI_106_C10	sucrose synthase (EC 2.4.1.13)	1.3			1	8	
NXCI_106_H10	cell division control protein 12 (septin)	1.3			1		17
NXCI_108_B11	UDP-glucose pyrophosphorylase	-1.3			7		
NXCI_108_E05	nucleoid DNA-binding-like protein	1.3			1		
NXCI_114_A11	no hit			1.3	5		22
NXCI_114_H07	putative uridylate kin	1.4			1		
NXCI_115_C04	putative glycosyl transferase	1.3			1		
NXCI_115_E10	nuclear RNA binding protein	-1.3	-1.3		5		

NXCI_116_D01	2-dehydro-3-deoxyphosphoheptonate aldolase		-1.3			4	9	
NXCI_117_C07	no hit				1.5	1		19
NXCI_117_D08	3-dehydroquinate dehydratase (EC 4.2.1.10)				1.3	1		19
NXCI_122_A09	enolase (EC 4.2.1.11)				1.4		9	19
NXCI_122_H05	adenosylhomocysteinase (EC 3.3.1.1)			1.2	1.8	4	12	16
NXCI_123_C05	acyl carrier protein, mitochondrial precursor	1.3				1		19
NXCI_124_C07	proteinase inhibitor	1.2			1.3	1		16
NXCI_124_E12	transporter	1.3				1		23
NXCI_125_F11	pectate lyase 2				1.9	1		19
NXCI_125_G03	1-aminocyclopropane-1-carboxylate				1.4	1		19
NXCI_126_B11	putative scarecrow	1.3				1		
NXCI_128_H10	unknown				-1.4			17
NXCI_130_A04	ribosomal protein	1.3				1		
NXCI_130_C09	tubulin beta	1.3				1		
NXCI_132_B11	26S proteasome subunit	1.2				1		
NXCI_132_E09	myb-related transcription factor	1.3			1.3	1		16
NXCI_132_H04	water stress inducible protein				-2.4	5		17
NXCI_135_H12	water stress inducible protein				-2.3	1		17
NXCI_136_A08	putative basic blue protein	1.2			-1.5	3		17
NXCI_137_B03	no hit	1.3			1.3	1		16
NXCI_137_D01	no hit	1.3				1		
NXCI_149_C10	anthranilate n-benzoyltransferase		1.4		1.8		12	19
NXCI_149_F01	thioredoxin H-type				1.5			19
NXCI_151_E08	acid phosphatase-like	1.3				1		
NXCI_153_G06	heat shock protein 70		1.3		1.3	1.6	12	16
NXCI_155_E06	transketolase (EC 2.2.1.1)				-1.4			17
NXCI_155_G05	no hit				-2.1	6		17
NXCI_156_D10	putative auxin-induced	-1.3				4		
NXCI_157_C11	no hit				-1.4			17
NXCI_164_F05	DNA-binding protein	1.3	1.3		1.3	1	10	19

NXCI_165_B06	RNA-binding like protein	1.3				1	22
NXCI_165_H04	cinnamoyl coa reductase8			1.7			19
NXLV082_F03	endo-beta-1,4-glucanase						
NXLV123_A09	xyloglucan endo-transglycosylase		1.3	1.6		12	19
NXLV127_E03	Glycoside transferase		1.3	1.3		10	19
NXNV_002_F08	ELONGATION FACTOR-1 ALPHA	1.3				1	
NXNV_005_B04	chloroplast nucleoid DNA binding			1.4		1	10 19
NXNV_008_F05	S-adenosylmethionine synthetase			1.7		3	12 19
NXNV_010_D03	calreticulin	1.3				1	
NXNV_010_H01	heat shock protein	1.3				1	
NXNV_012_H01	TIR/P-loop/LRR	1.3				1	
NXNV_027_E09	Avr9 elicitor response protein-like			1.3		1	16
NXNV_031_G03	peroxidase (EC 1.11.1.7)			1.6		1	19
NXNV_044_B12	scarecrow-like 1 (transcription factor)	1.3			-1.2	3	18
NXNV_044_E12	fiber protein		1.4			2	10
NXNV_044_F10	no hit			2.1			19
NXNV_046_H05	putative arabinogalactan protein		1.5	3.7		3	12 19
NXNV_047_B11	hypothetical protein	1.2				1	
NXNV_056_F03	putative disease resistance protein	1.3		1.3		1	18
NXNV_060_D05	putative fatty acid elongase		1.4				12 18
NXNV_060_H10	3-phosphoshikimate carboxyvinyltransferase	1- 1.3				1	
NXNV_061_B02	no hit			1.4			16
NXNV_063_B09	carboxypeptidase C (EC 3.4.16.5)	-1.3				5	
NXNV_064_D11	adenosylhomocysteinase (EC 3.3.1.1)	1.2				1	
NXNV_064_E06	putative phi-1-like phosphate-induced protein			-1.3		3	17
NXNV_065_C04	similar to stress responsive lectin-like cDNAs from rice			-1.2			22
NXNV_065_D01	thioredoxin-like	1.3				1	
NXNV_066_A07	xyloglucan endotransglycosylase	1.3				1	
NXNV_066_B07	laccase (diphenol oxidase)	1.2		3.9		1	19
NXNV_066_D07	no hit		-1.5	-1.3	-2.0	5	11 17

NXNV_066_E09	phenylcoumaran benzylic ether reductase					1.7		12	19
NXNV_067_B05	laccase (diphenol oxidase)					2.4		12	19
NXNV_067_G03	nucleotide pyrophosphatase homolog	1.3				1.3	1		19
NXNV_072_C01	no hit					-1.4			17
NXNV_073_F11	no hit				-1.3			11	
NXNV_073_G08	protein translation inhibitor		-1.3				7		
NXNV_074_D01	galactose-1-phosphate uridylyltransferase	1.3					1		
NXNV_074_F12	unknown	1.3					1		
NXNV_074_G01	zinc finger protein	1.3					1		
NXNV_074_G06	no hit	1.3					1		
NXNV_074_G09	putative bZIP transcription factor	1.3					1		
NXNV_077_C07	14-3-3 protein	1.4					3		
NXNV_081_A09	calmodulin		1.3			1.3		10	19
NXNV_081_D10	no hit			1.4		1.4	1	12	19
NXNV_083_A10	cinnamyl alcohol dehydrogenase			1.6		1.8		12	19
NXNV_083_E04	methionine synthase					1.3			19
NXNV_083_H11	BAX inhibitor-1 like					-1.6	7		17
NXNV_085_G09	vesicle-associated membrane protein		1.3					10	
NXNV_089_A02	no hit	1.2					1		
NXNV_089_B08	tubulin beta chain					-1.4			17
NXNV_091_A04	pectin methylesterase isoform alpha					1.7	1		19
NXNV_091_F02	cytochrome-c oxidase (EC 1.9.3.1) chain I			1.3				12	
NXNV_092_A07	putative isoprenylated protein	1.3					1		
NXNV_094_C11	histone H2b	1.3					1		
NXNV_094_E09	signal peptidase		1.3			1.3		10	19
NXNV_096_C08	intracellular pathogenesis-related protein		-1.2	1.3		-1.6	1.3	12	22
NXNV_096_C09	asparagine synthetase type II			1.3		-1.2	1.4	12	22
NXNV_096_G04	argonaute	-1.3					4		
NXNV_098_D05	NADH dehydrogenase (ubiquinone)					1.9			19

NXNV_098_G03	potassium transport protein kt				-1.7			17
NXNV_100_G12	no hit				1.3			19
NXNV_103_C02	cell division cycle protein		1.3				10	
NXNV_103_G03	no hit	-1.2					7	
NXNV_103_H09	histone H2A	1.3					1	
NXNV_106_A05	methionine synthase		1.2					12
NXNV_106_A11	endo-1,4-beta-glucanase				-1.5			17
NXNV_106_C07	Beta-xylosidase		1.3					10
NXNV_106_E08	protein serine/threonine phosphatase		1.3					10
NXNV_106_F12	pollen major allergen				-1.3			17
NXNV_108_E09	60S ribosomal protein	1.3					1	
NXNV_117_F02	glyceraldehyde 3-phosphate dehydrogenase		1.5					12
NXNV_118_C02	putative transcription factor	1.2					1	
NXNV_120_B01	receptor kinase (CLV1)	1.2					1	
NXNV_120_C02	cellulase (EC 3.2.1.4)	-1.2					5	
NXNV_122_C07	phototropin 2				-1.3			11
NXNV_124_C02	triosephosphate isomerase, cytosolic	1.3					1	
NXNV_125_E04	no hit	1.3			1.3		1	16
NXNV_125_G04	no hit				1.3	1.7	1	18
NXNV_127_E04	isoflavone reductase homolog	1.3					1	
NXNV_128_D10	Ubiquitin ligase		1.6			1.3		10
NXNV_129_A06	no hit	1.4					1	
NXNV_129_E04	no hit			-1.3		-2.0	7	17
NXNV_129_F09	vacuolar H ⁺ ATPase subunit E	1.3					1	
NXNV_132_G06	endoglucanase 1 (ec 3.2.1.4) (endo-1,4-beta-glucanase) (cellulase)		1.4				3	10
NXNV_132_H07	similar to stress responsive lectin-like cDNAs from rice		1.5					10
NXNV_132_H12	TIR/NBS/LRR disease resistance protein				1.3		3	19
NXNV_133_D04	early response to drought 3				1.3	1.7	4	16
NXNV_134_A05	putative type 1 membrane protein		1.5					10

NXNV_134_H10	no hit	-1.4	-1.3		1.4	-1.5	7		17
NXNV_136_F10	LACCASE (EC 1.10.3.2)	1.3				1.2	1		16
NXNV_139_A05	no hit			1.3			1	10	19
NXNV_143_B10	no hit					1.4	1		19
NXNV_146_G08	disease resistance protein, putative					-1.3			17
NXNV_147_G04	RNA-binding protein	1.3					1		
NXNV_148_H07	disease resistance protein-like					-1.3			17
NXNV_153_F09	basic blue protein					-1.5	1	8	17
NXNV_153_H09	peroxidase (EC 1.11.1.7) precursor, cationic			1.3			1	12	16
NXNV_154_B07	AMP-binding protein					1.3	1		19
NXNV_154_G11	no hit	1.3				1.4	1		16
NXNV_158_A11	methylenetetrahydrofolate reductase					1.6	6		19
NXNV_158_B11	cysteine proteinase					-1.4	7		17
NXNV_160_C09	pre-mRNA splicing factor prp19			-1.3				8	
NXNV_162_H07	thioredoxin H-type					-2.1	4		17
NXNV_164_D05	IAA-ALA hydrolase					1.6			19
NXNV_164_G08	3-deoxy-d-arabino-heptulosonate 7-phosphate synthetase			1.4			3	12	
NXNV_164_H08	putative xyloglucan endotransglycosylase					-1.7	1.3		17
NXNV_165_G01	methionine synthase			1.4		1.2	1	10	19
NXNV_181_B11	cellulose synthase (EC 2.4.1.-)					1.3	2		19
NXNV_185_H03	dehydroquinase shikimate dehydrogenase					1.4			19
NXNV_186_D04	putative receptor-like	1.3					1		
NXNV_186_D12	ring zinc finger protein					-1.5			17
NXNV_187_B04	CDC2PNC PROTEIN	-1.3					7		21
NXNV_187_D12	putative ubiquitin conjugating enzyme	-1.3					4		
NXNV_187_F06	XET precursor					1.2			18
NXNV027B07	cellulose synthase					-2.1			17
NXNV047B05	cellulose synthase					-1.2			17
NXPV_011_C08	putative disease resistance protein					-1.9			17

NXPV_013_C08	disease resistance protein, putative									-3.0	14	17				
NXPV_037_C02	resistance protein - like									-1.6		17				
NXPV_037_H03	RPP1 disease resistance protein - like									1.5		19				
NXPV_038_A07	xyloglucan endotransglycosylase									1.6		19				
NXPV_038_C08	MtN21 nodulin protein-like									-1.4	-3.1	11	17			
NXPV_041_F10	disease resistance protein-like									1.4	1.5	12	19			
NXPV_043_G04	MtN21 nodulin protein-like									-1.4	-1.2	-3.1	11	17		
NXPV_055_C02	beta-glucosidase like protein										-1.7		17			
NXPV_066_G12	putative disease resistance response protein										-1.7		17			
NXPV_067_A08	xyloglucan endotransglycosylase										-1.6		17			
NXPV_069_B02	disease resistance protein EDS1									1.3		12	18			
NXPV_084_H10	putative disease resistance protein										-1.2	-3.0	17			
NXPV_088_C08	xyloglucan endo-transglycosylase										-1.6	1.3	17			
NXPV_101_D06	disease resistance protein										-1.5		17			
NXR061_H10	xyloglucan endotransglycosylase										-1.4		17			
NXR064_C07	xyloglucan endotransglycosylase									1.3		14	17			
NXR072_A01	cellulose synthase										-1.3		17			
NXR077_E01	hypothetical protein										1.3		19			
NXR079_D01	xyloglucan endotransglycosylase XET1										-1.5		17			
NXSI_001_G04	no hit										-1.3	-1.4	7			
NXSI_005_F10	no hit										-1.3	-1.3	7			
NXSI_007_H12	sucrose synthase										-1.3		5			
NXSI_008_C03	probable MADS box protein MADS8										1.2		16			
NXSI_008_D10	laccase (diphenol oxidase)										1.9		19			
NXSI_012_D03	photosystem ii 10 kDa polypeptide precursor										-1.8	1	17			
NXSI_012_D08	probable peroxidase (EC 1.11.1.7)									1.4	3.0	1.3	3.4	6	12	19
NXSI_012_H05	s-adenosylmethionine synthetase										1.7	1.2	1.7	6	12	16
NXSI_012_H11	malate synthase-like protein											1.7			19	
NXSI_013_B10	pinoresinol-lariciresinol reductase										1.8	1.7		12	19	
NXSI_021_A09	CLAVATA1 receptor kinase (CLV1)-									1.2	1.4	-1.3		3	10	17

	like								
NXSI_021_D01	no hit					-1.5		4	17
NXSI_021_E09	2-oxoglutarate/malate translocator-like protein					1.3			19
NXSI_023_B04	probable high mobility group protein HMG1	-1.3						7	18
NXSI_023_E09	ascorbate peroxidase	-1.3						4	
NXSI_024_C02	homeobox transcription factor KN3	1.2						3	
NXSI_025_H02	alpha-pinene synthase					-1.4		1	17
NXSI_026_G02	no hit	1.3						1	
NXSI_026_H06	similar to stress responsive lectin-like cDNAs from rice					-1.4			17
NXSI_027_G10	5-methyltetrahydropteroyltriglutamate--homocysteine s-methyltransferase (methionine synthase 2)(rice)					1.7			19
NXSI_028_B10	peroxidase ATP 4 (EC 1.11.1.7)		1.4	2.3		4.8		6	12 19
NXSI_029_D04	lactoylglutathione lyase (ec 4.4.1.5)	1.3						3	
NXSI_030_C06	calcium binding protein	1.3				1.3	1.4	1	11 17
NXSI_030_D05	protein transport protein sec61 alpha subunit	-1.3						4	
NXSI_031_E03	1,4-benzoquinone reductase-like, TRP repressor.	-1.2						7	
NXSI_031_H03	serine carboxypeptidase III precursor	-1.3						5	
NXSI_031_H06	phosphoglycerate kinase			1.3		1.3			12 19
NXSI_036_H01	protein binding / signal transducer	1.4						1	
NXSI_039_E06	MADS box transcription factor					1.3		1	19
NXSI_039_G02	disease resistance protein-like			1.5					10 19
NXSI_039_G09	no hit	1.3						1	
NXSI_040_C01	no hit			1.2					10
NXSI_040_D02	putative arabinogalactan protein		-1.3					7	21
NXSI_040_H09	phosphogluconate dehydrogenase (decarboxylatin... 286 1e-76)	-1.3						5	12

NXSI_041_A07	senescence-associated protein homolog					1.3		1	19
NXSI_047_H09	nicotianamine synthase (EC 2.5.1.43)	1.3						1	
NXSI_048_D06	malate dehydrogenase, cytoplasmic 1	-1.3						7	
NXSI_048_H03	histone-like protein	-1.5						5	
NXSI_049_A01	thaumatin-like protein					-1.3			17
NXSI_051_B09	no hit			1.3		1.8		12	19
NXSI_052_A11	putative RNA binding protein	-1.3						4	
NXSI_052_B04	valine--tRNA ligase-like protein	-1.2						7	
NXSI_052_E09	NBS/LRR disease resistance protein	-1.3						5	
NXSI_053_D09	no hit			1.4		1.3			10 19
NXSI_054_F05	glycine-rich protein					1.5	1.3		21
NXSI_055_B06	gasa5-like protein.					1.5			15 16
NXSI_055_F08	putative auxin-induced protein			1.4				6	12
NXSI_055_F10	aquaporin	-1.3	-1.3			-1.5		7	14 17
NXSI_057_C07	translation initiation factor eIF-4	-1.2						4	
NXSI_060_B07	expansin					1.3			16
NXSI_061_A07	no hit					1.2			19
NXSI_063_D01	naringenin,2-oxoglutarate dioxygenase	3- -1.2						5	20
NXSI_063_G10	CDC2 cykline dependent kinase					-1.4			17
NXSI_064_A03	thaumatin		1.5	1.3	1.9	3.0		6	12 19
NXSI_064_A08	no hit	1.2						3	
NXSI_064_B03	cytochrome b5 isoform Cb-5					1.4			16
NXSI_065_B06	glycine hydroxymethyltransferase (EC 2.1.2.1)			1.3				6	10
NXSI_066_A02	2-oxoglutarate dehydrogenase			1.3				7	10
NXSI_066_E05	tonoplast intrinsic protein bobtip					-1.5			17
NXSI_067_B12	no hit	-1.3						4	
NXSI_068_G09	glyceraldehyde 3-phosphate dehydrogenase					-1.3			17
NXSI_070_H07	blue copper protein precursor	-1.3						4	
NXSI_076_A12	putative seed storage protein (vicilin)					1.3			19

NXSI_107_G10	temperature induced lipocalin			-1.5				17
NXSI_108_C10	ubiquinol--cytochrome-c reductase	-1.3				7	8	
NXSI_108_D12	5- methyltetrahydropteroyltriglutamate-- homocysteine S-methyltransferase (methionine synthase 2)(rice)			1.6			12	19
NXSI_109_B12	hypothetical protein		1.3				2	
NXSI_110_A07	Argonaute (AGO1)-like protein	-1.3					5	
NXSI_110_C12	gamma tubulin		1.3					10
NXSI_112_B07	aquaporin, tonoplast intrinsic protein	-1.2		-2.1		7		17
NXSI_112_D01	no hit		1.2			1	10	19
NXSI_113_E06	xyloglucan endo-transglycosylase			-1.5	1.3			17
NXSI_113_G12	quinone oxidoreductase homolog	-1.3				5		
NXSI_114_A04	no hit			1.7				19
NXSI_114_E07	aldehyde dehydrogenase			1.3				19
NXSI_115_A12	translation initiation factor			-1.4				11
NXSI_115_E04	proteasome epsilon chain precursor	-1.3					4	
NXSI_116_E07	ribosomal protein		1.3				4	10
NXSI_116_F02	hexokinase (EC 2.7.1.1) 1	1.3				1		
NXSI_116_G04	photoassimilate-responsive protein		1.4		1.3		10	19
NXSI_116_G10	putative vacuolar proton-ATPase subunit	1.3				1		20
NXSI_117_B05	alcohol dehydrogenase		1.3				6	12
NXSI_117_C01	no hit		1.4					10
NXSI_118_C03	ring zinc finger protein-like		1.3					12
NXSI_121_B09	protein kinase/proteine serine/threonine kinase	1.3				1		
NXSI_121_D02	vacuolar ATP synthase catalytic subunit	-1.2					2	
NXSI_121_H06	chitinase 1 precursor			1.7				19
NXSI_122_A12	no hit		1.3				2	
NXSI_125_D03	similarity to RNA binding protein	-1.2					7	
NXSI_126_A06	no hit			-1.3				14

NXSI_127_C02	laccase		1.3		1.8	6	10	19
NXSI_127_E09	disease resistance protein-like				-1.6			17
NXSI_128_E05	copper chaperone homolog		1.4		1.3		10	19
NXSI_128_E08	DNAJ protein homolog		1.4		1.2		10	19
NXSI_128_G02	ATP synthase delta chain, mitochondrial protein	-1.2				7		
NXSI_129_E10	phosphoenolpyruvate carboxykinase				1.3			16
NXSI_131_C03	putative aba induced plasma membrane protein		-1.3		-1.5	1	8	17
NXSI_132_B10	lanatoside 15'-O-acetylerase precursor	-1.3				7		
NXSI_133_F03	flavonol glucosyltransferase				-1.4			17
NXSI_134_C01	glyceraldehyde 3-phosphate dehydrogenase				-1.5			17
NXSI_134_E09	pectate lyase				1.5			16
NXSI_134_F04	endo-beta-1,4-glucanase		-1.2			1		
NXSI_135_B02	glycosylation enzyme-like protein		1.5				10	19
NXSI_137_D09	no hit			-1.2		5	11	
NXSI_138_H05	60S ribosomal protein-like				1.3			19
NXSI_139_B08	nucleoside diphosphate kinase i	-1.2				7		
NXSI_139_G02	18.2 kDa class i heat shock protein	1.2				1		
NXSI_141_G01	Receptor protein kinase-like protein		1.3			3	10	
NXSI_142_E03	glutathione transferase (EC 2.5.1.18)		1.5			4	12	
NXSI_142_F05	histone-like protein			-1.4		7	11	
NXSI_142_F10	transcription factor Hap5a-like protein	1.3				1		
NXSI_143_G06	leucine-rich repeat protein		1.2			4	12	
PC_04_B12	transcription factor	1.3			1.3	1		16
PC_04_G10	floral homeotic protein	1.3			1.3	1		16
PC_05_A11	late embryogenesis abundant protein				1.3			18
PC_08_F08	LEA76 homologue type2	1.3				1		16
PC_08_H11	no hit	1.3				1		18
PC_10_A05	lipid transfer protein				1.3	3		16
PC_10_C02	LEA76 homologue type2	1.2			1.3	1		18

PC_11_C08	LEA76 homologue type2	-1.2			7	16
PC_13_G09	WUSCHEL (transcription factor)	1.3		1.4	1	16
PC_14_C08	late embryogenesis abundant protein			1.3	1	16
PC_23_D04	LEA76 homologue type2	1.3			3	18
ST_01_E01	CAAX amino terminal protease-like protein			1.3	1	16
ST_06_D06	putative receptor kinase	1.2			1	
ST_06_F05	fiddlehead protein			1.3		16
ST_08_A10	no hit			1.5		9 19
ST_17_B05	chromodomain-helicase-DNA-binding protein	1.2			1	18
ST_21_E01	fad binding / aldehyde-lyase/ oxidoreductase/ oxidoreductase, acting on ch-oh group of donors			-1.6		8 17
ST_23_F07	ATP-citrate-lyase		1.4	1.6		12 19
ST_23_G07	putative auxin-induced protein	-1.4			4	
ST_25_D09	auxin response factor	1.3			1	
ST_29_G04	putative zinc finger protein		1.3		3	18
ST_31_D06	glutathione s-transferase			1.6		12
ST_32_C09	late embryogenesis abundant protein		1.2		2	
ST_35_A01	metallothionein-like protein			1.8		19
ST_40_A03	porine MIP1			-1.3		17

*The genes were determined by the microarray to be differentially expressed if the fold change was ≥ 1.2 or ≤ -1.2 . All the genes were divided into 23 regulatory patterns, indicated by the numbers 1-23 (there was no gene with fold change above the 1.2 threshold belonging to pattern 13).

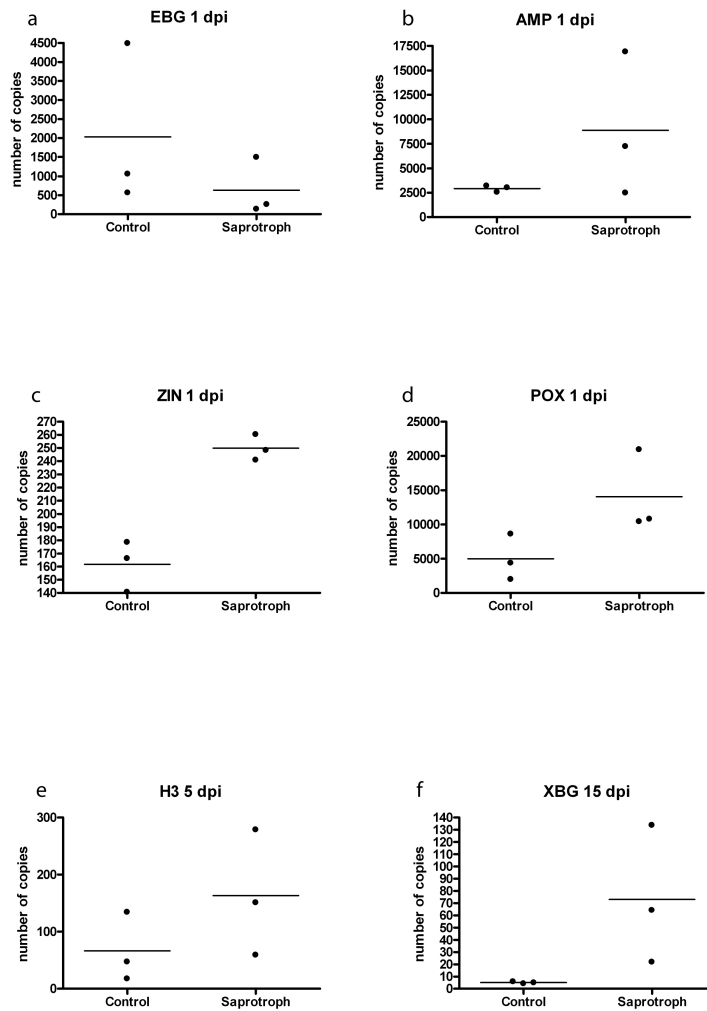


Figure S1 a-f. Distribution of number of transcripts determined by real-time RT-PCR in control pine roots and infected with *H. annosum* at 1, 5 or 15 d.p.i. Each dot represents a biological replicate consisting of three technical replicates. Bar represents mean copy number. Abbreviations: AMP - antimicrobial peptide, EBG - endo-beta-1,4-glucanase, H3 - histone H3, POX - peroxidase, XBG - xyloglucan endotransglycosylase, ZIN - zinc finger protein.

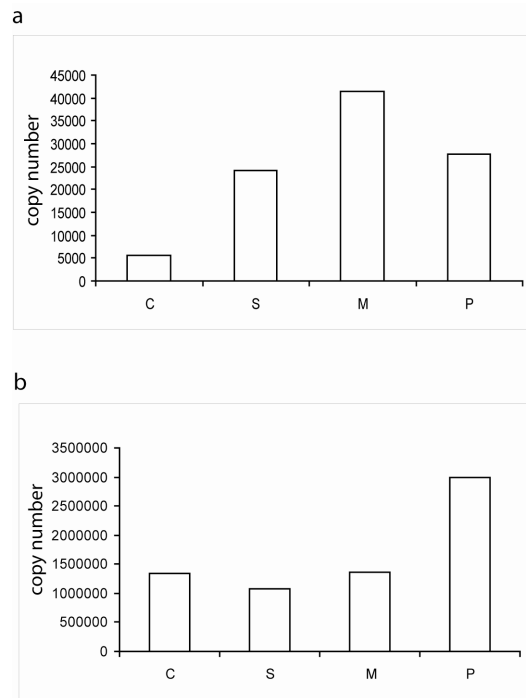


Figure S2. Expression of antimicrobial peptide (AMP) determined by real-time RT-PCR in control (C) *P. sylvestris* roots and challenged with *L. bicolor* (M), *H. annosum* (P) or *T. aureoviride* (S) at a) 1 and b) 5 d.p.i.